AN ABSTRACT OF THE THESIS OF

LEE, YONG-INN for the degree of DOCTOR OF PHILOSOPHY

in PHYSICS presented on November 27, 1984

Title : COLLECTIVE ELECTRONIC EXCITATION MODES IN A SUPERLATTICE

Abstract approved: Redacted for privacy

Allen Wasserman

Collective excitation(plasmon) modes of an electron gas in a multilayer system (superlattice) have been studied in great detail in recent years. One important aspect of this Fermion system is that the dispersion relation of the plasma frequency shows transitional behavior between two- and three- dimensional character. Inelastic light scattering experiment has recently been conducted, in which the intermediate dispersion was observed for a superlattice. The results of the light scattering experiment and earlier calculations based on a superlattice of two dimensional layers model developed by Fetter and Das Sarma and Quinn are in qualitatively good agreement. Nevertheless there are discrepancies between this theory and experiment, especially for increasing values of q. The objective of this work is to improve Fetter and Das Sarma and Quinn's theory to include the effect of finite thickness of the plasma layers with the objective of better understand-

ing the systematic discrepancy and to describe electronic correlations in a superlattice in a more general way. It proceeds by the determination of the particle-hole channel of the two particle Green's function in the Random Phase Approximation. The problem is examined here in the two band limit with the envelope functions of the infinite square well potential for both the plasmon and resonant screened single particle excitations. The results are in quantitatively excellent agreement with the experiment.

COLLECTIVE ELECTRONIC EXCITATION MODES IN A SUPERLATTICE

by

LEE, YONG-INN

A THESIS

submitted to

Oregon State University

in partial fulfillment of

the requirements for the

degree of

Doctor of Philosophy

completed January 16, 1985

Commencement June 1985

APPROVED:

Redacted for privacy

Associate Professor of Physics

in charge of Major

Redacted for privacy

Chairman of Department of Physics

Redacted for privacy

Dean of Graduate School

Date thesis is presented November 27, 1984

Typed by Kathy Haag for Lee, YONG-INN

TABLE OF CONTENTS

List of Figures

List of Figures --- continued

List of Figures--- continued

List of Tables

COLLECTIVE ELECTRONIC EXCITATION MODES IN A SUPERLATTICE

Chapter I

INTRODUCTION

A. SUPERLATTICES: Initial Remarks

A superlattice arises when a periodic one dimensional spatial modulation is imposed on a three dimensional system. A simple form of superlattice is created by a periodic displacement field of ultrasonic waves applied along one crystal direction (1). A more complex superlattice can be produced by epitaxial growth of crystals with periodic variation of alloy composition. Typical materials used in this way are GaAs and GaAs alloys which are n- and p- doped to form periodic array of heterojunctions. Superlattices may also be made from a periodic array of n-doped, intrinsic and p-doped layers of an otherwise homogeneous three dimensional semiconducting material (2). These relatively primitive superlattices have largely been replaced by a new generaiton of structures made possible by the recent development of molecular beam epitaxy (MBE). Currently MBE allows high quality artificial superlattices with atomically sharp boundaries to be made

from different semiconductor materials with similar lattice structures and matching lattice parameters. Typical semiconductors used in this process are InAs-GaSb and GaAs-AlAs.

Superlattices differ from homogeneous bulk materials because the superlattice potential created by periodic heterojunctions modifies significantly the band structure of the host semiconductors by creating energy subbands and minizones in wave vector space. The superlattice, not present in nature, can be designed to exhibit unusual electronic and optical properties somewhat intermediate between the materials that create the modulated structure by an appropriate choice of semiconductors and of the width of their layers. In addition dimensionality behavior "intermediate" between two and three dimensions is also exhibited. "Intermediate" dimensionality is illustrated by electron plasma oscillations in the superlattice. The term intermediate is used here without any implication of dimensional scaling but only to suggest a consequence of the superlattice which causes behavior that differs from either the 3-dimension or 2-dimensional bulk material. Specifically, for a three dimensional system the long wavelength collective electronic modes have an energy spectrum that behaves according to

$$\omega_p = \left(\frac{4\pi ne^2}{\varepsilon_0 m}\right) \qquad \text{(C.G.S.)} \qquad (1.1)$$

where

n: volume charge density

m: effective mass of electron

ε_0: background static dielectric constants

which is independent of the wavevector Q(3,4). On the other hand a true two dimensional plasma (i.e. a single infinitely thin plasma layer) has an excitation spectrum that behaves according to

$$\omega_p \sim \sqrt{Q} \qquad (1.2)$$

where

wave vector $\vec{Q} = (\vec{q}, 0)$

(This result, first demonstrated by Stern (5), is not so familiar as the 3-dimensional case and for completeness is derived in detail in Appendix A.) Finally, in a superlattice of alternating 2-dimensional plasma layers separated by insulating layers, the plasma frequency is affected by periodic electronic correlations between different layers and (6,7).

$$\omega_p \sim Q \qquad (1.3)$$

These plasma oscillations of intermediate dimensionality can in fact be experimentally studied by inelastically scattering light from the surface of a superlattice at a frequency such that the insulating layers are nearly transparent to the light (8). In this experiment a non-resonant spectral cross section for light scattered by plasmons is observed and enables one to measure the dispersion relation of these superlattice plasmons.

The question of intermediate dimensionality has been considered in theoretical work of Fetter (7) and Das Sarma and Quinn (6), both of whom treat the plasma layer as 2-dimensional plasma sheet. Fetter and Das Sarma and Quinn (DSQ)are in good qualitative agreement with the experimental results (8). apart from a small but systematic discrepancy. The question of intermediate dimensionality is of sufficient interest that the major part of this thesis is to improve DSQ theory to include the effect of finite thickness of the plasma layers with the object of better understanding the systematic discrepancy and to describe electronic correlations in a superlattice in a more general way.

B. SUPERLATTICES: Type I and Type II

Two types of superlattices have been studied in great detail. The Type I system, typified by GaAs-$Al_xGa_{1-x}As$, is a heterogap system where the band gap of GaAs is contained entirely within the band gap of $Al_xGa_{1-x}As$. giving rise to band gap discontinuities in both the conduction and valence bands of the resultant superlattice system (9). The band gap arrangement of a type I system is illustrated in Fig. 1(a). Approximately 85% of the change in energy gap occurs in the conduction band edge and 15% in the valence band edge (see Appendix B) (10,11). The band gap discontinuities at the interface of the two materials are most simply thought of as potential wells in the conduction and valence bands caused by potential barriers from the $Al_xGa_{1-x}As$ which separate GaAs layers. Selective doping of the $Al_xGa_{1-x}As$ layers produces ionized donors in these layers and the electrons released by these donors migrate into the potential well on the GaAs side. The periodic one-dimensional potential well perpendicular to the superlattice layers quantizes the electronic motion along the superlattice direction, and the conduction band (GaAs) splits into a series of subbands, each of which represents effective mass type electronic motion in the plane perpendicular to the superlattice direction.

The Type II superlattice system is typified by an InAs-GaSb alloy system with a typical band configuration as illustrated in Fig. 1(b). In the Type II superlattice it is even possible that the conduction band minimum of InAs may be lower than the valence band maximum of $GaSb_{1-y}As_y$(9). It is a distinctive characteristic of type II superlattice systems that a spatial separation of electrons and holes takes place due to a transfer of holes to GaSb and electrons to InAs. In contrast, in the type I system both electron and hole states are primarily confined in the GaAs regions. Electron and hole occupation is indicated by the shaded and cross hatched areas respectively in Fig. 1. The spatial separation has obvious consequences in optical properties such as absorption and carrier life times (9). For example, the electron-hole recombination amplitude is proportional to the overlap integral between their associated envelope wavefunctions and will therefore be small if the electron and hole wave functions peak in spatially different regions. Transitions between subbands localized in different layers of type II systems can be observed only in thin layered superlattices where wavefunction penetration into neighboring regions is significant.

C. SUPERLATTICES: Doping

Superlattices are generally (i) uniformly doped (UD) with both components identically doped with donors such as Si, or (ii) modulation doped (MD) with the Si and Al source fluxes in MBE so synchronized that only the $Al_xGa_{1-x}As$ layers are deliberately doped with Si. (If Si diffusion is negligible at the growth temperature of 600 C, then the GaAs layers will contain only a background impurity concentration much less than the doping levels in $Al_xGa_{1-x}As$). In yet another MD technique, the Si beam is shuttered in such a way that up to 60 Å of each side of every $Al_xGa_{1-x}As$ layer is not intentionally doped, thus keeping the Si dopant away from the interface region. Fig. 2 presents a model for the electronic level structure of a UD and MD superlattice. Note that the electronic structure is complicated by the presence of space charging at the interfaces. Since the GaAs conduction band edge lies lower in energy than the $Al_xGa_{1-x}As$ donor states (refer to Fig. 2), electrons from the donors will migrate

into the GaAs regions to occupy GaAs subband states. In order to satisfy the requirement of a constant Fermi level throughout the superlattice the $Al_xGa_{1-x}As$ regions are electron depleted for both UD and MD structure. This in turn leads to space charge induced "band bending", the degree of which is both impurity concentration and layer thickness dependent. The higher the doping concentration the greater the expected space charge in the regions of depletion and accumulation, hence higher dipolar fields and band bending. This, in a self consistent fashion, confines electron wavefunctions toward the interface (see Fig. 3) (12).

Because of the periodicity of the boundary conditions, if the GaAs layer is thin the wavefunction will be perturbed such that a significant amplitude remains at the center of the quantum well. As the thickness of GaAs layer increases, periodicity becomes less significant and the amplitude of the wavefunction of the electron will be concentrated at the interface, as in a single junction. If the GaAs layer is very thick, the very large dipolar electric field at the junction will result in the strong band bending more typical of an isolated heterojunction.

The most important feature of the MD structure is that essentially all of the mobile carriers (electrons

confined to the GaAs layers) and their parent donor impurities (in the $Al_xGa_{1-x}As$ layers) are spatially separated from each other in an irreversible manner. Thus the electron density in the GaAs layer may greatly exceed the density of background impurity scattering centers leading to a highly enhanced carrier mobility in the low temperature where ionized impurity scattering mechanism is important. At high carrier density even this mechanism is reduced by screening.

Fig. 1. Schematic energy diagrams (a) for the Type 1 superlattice system (b) for the Type II superlattice system.

where

subscripts 1 and 2 are used to indicate the first and second host semiconductors. Subscripts c and v are used to indicate their conduction and valence bands. The quantum states or subbands are shown in horizontal lines; e and h refer to electrons and holes, and numericals in this case refer to the indices of subbands with 1 representing the ground states. The effective energy gap of the superlattice is defined as the energy difference between the ground subbands, $E_{gs} = E_{1e}-E_{1h}$. Shaded indicating electrons and cross-hatched indicating holes.

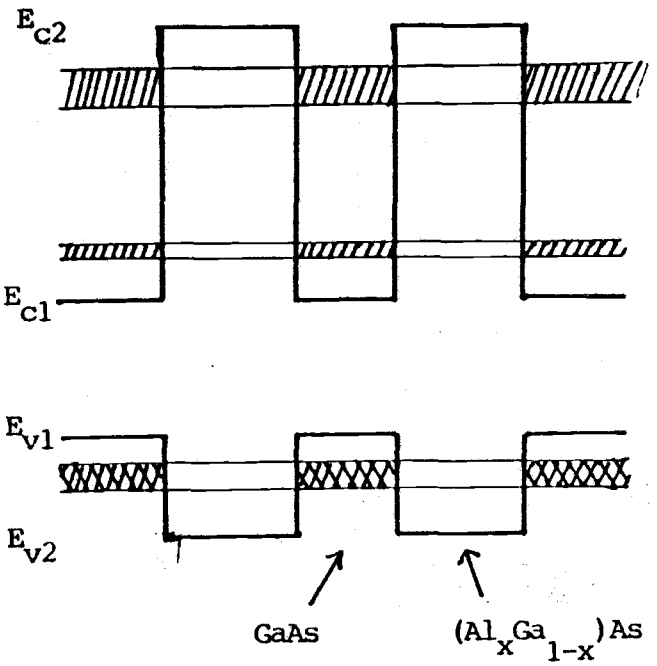
E_{c2}
E_{c1}
E_{v1}
E_{v2}
GaAs
$(Al_xGa_{1-x})As$

Fig. 1. (a)

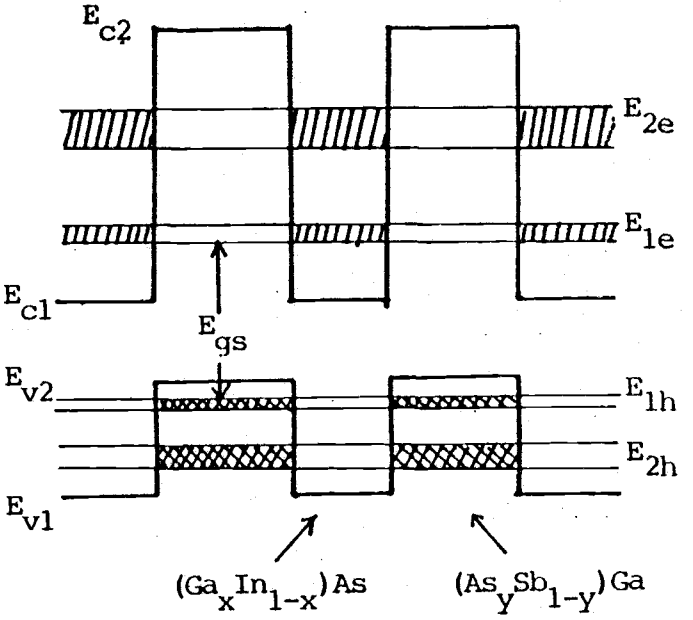
E_{c2}
E_{2e}
E_{1e}
E_{c1}
E_{gs}
E_{v2}
E_{1h}
E_{2h}
E_{v1}
$(Ga_xIn_{1-x})As$
$(As_ySb_{1-y})Ga$

(b)

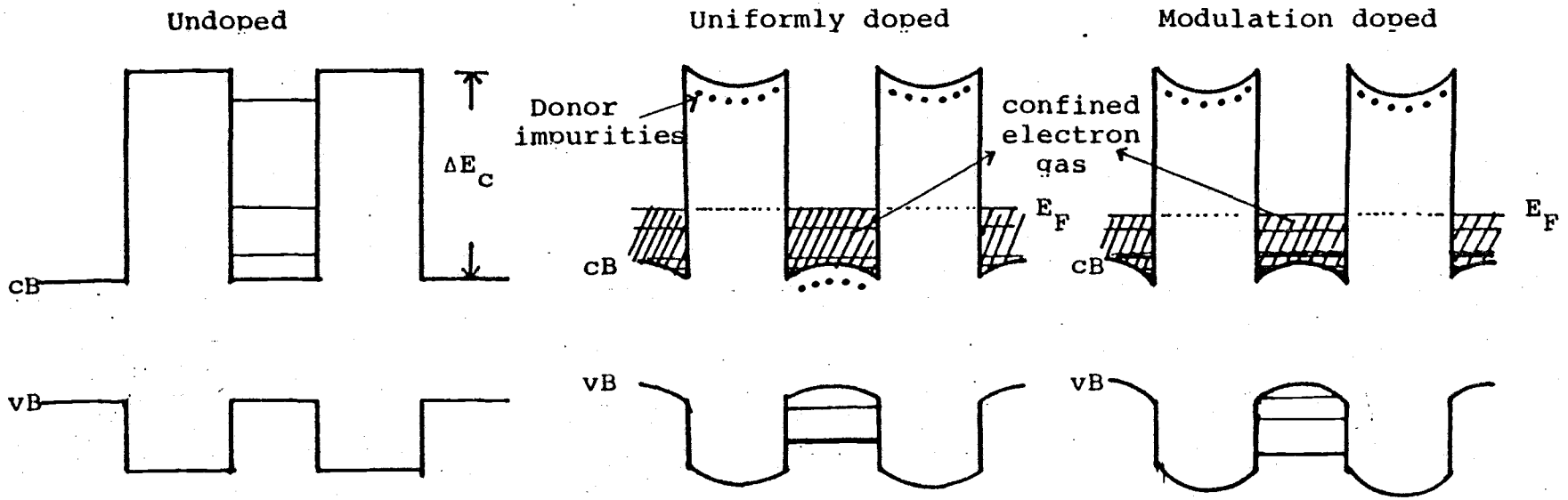

Fig. 2. Energy band diagrams for the n-doped and undoped GaAs-$(Al_xGa_{1-x})As$ superlattices. Typically $x \cong 0.3$ in $(Al_xGa_{1-x})As$, leading to $\Delta E_c = 300$ meV.

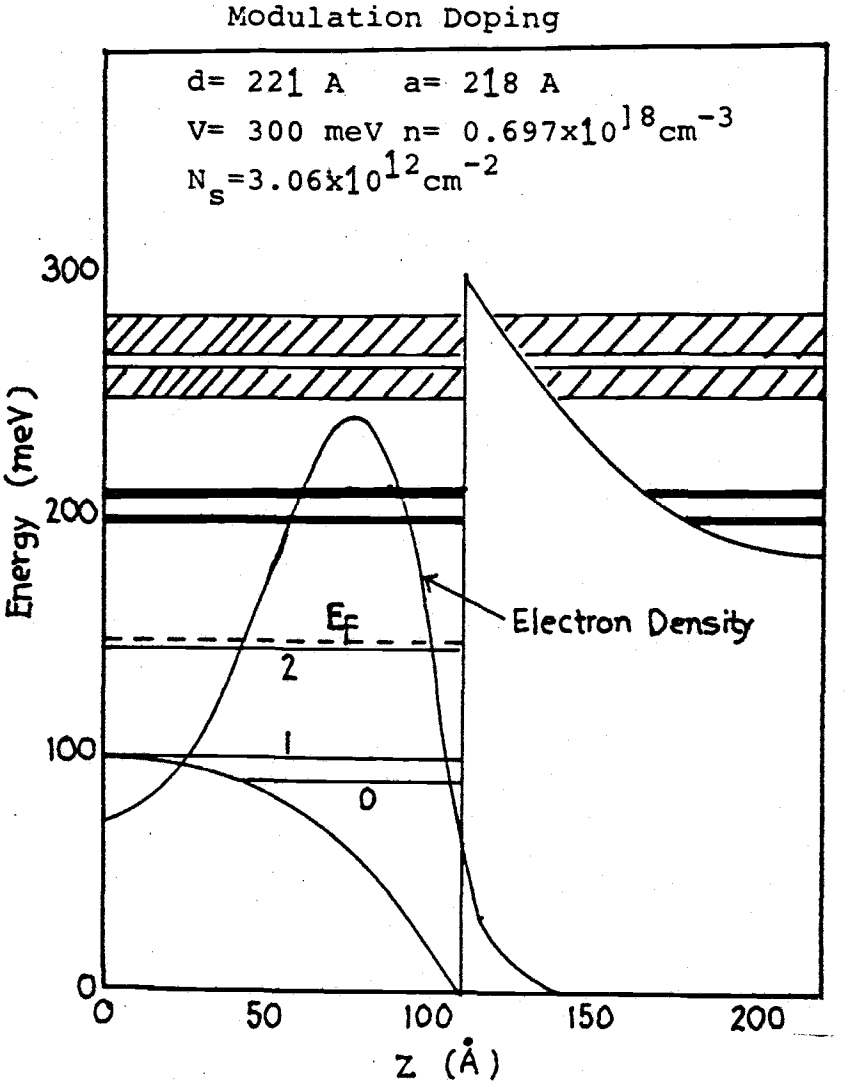

Fig.3. (a)

Calculated energy levels,density distribution of electrons and the self- consistent potential in the case of modulation doping. The subband widths are described by hatches.

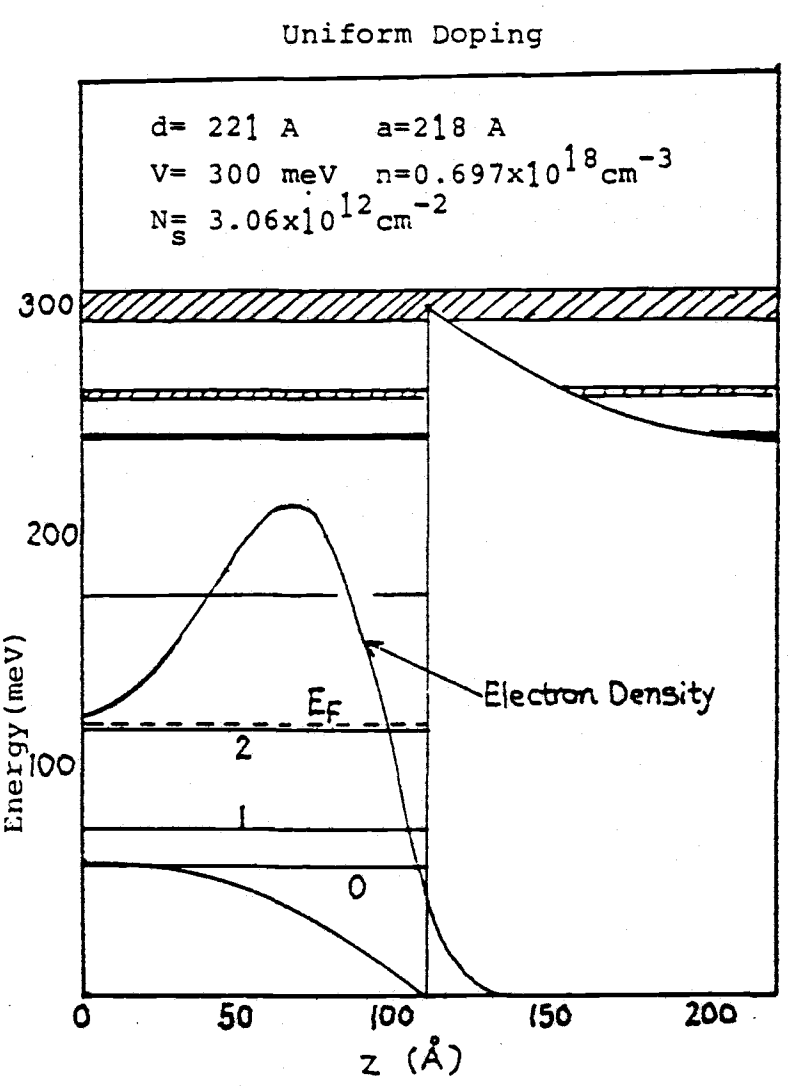

Fig.3. continued. (b)

Calculated energy levels, density distribution of electrons, and the self-consistent potential in the case of uniform doping. The subband widths are described by hatches.

Chapter II

GENERAL REMARKS ON THIS THESIS

An important aspect of interacting fermion systems are the plasma eigen modes which are the normal modes of the collective oscillations. The plasma modes are not only an interesting theoretical concept resulting from electron correlations but appear in optical properties such as absorption (13,14) and transmission (15), as well as light scattering (16,17), since they are the complex zeros of the dielectric response function (16,18,19).

The plasma mode which is a quantized charge density fluctuation is generally well defined only at small wave vectors, beyond which it decays into particle-hole pairs. Thus the plasma mode, not unlike quantized lattice density fluctuations (phonon), are amenable to classical theoretical treatments. The superlattice calculation of Fetter and DSQ are essentially a classical treatment which ignores all quantum mechanical features such as subbands and subband mixing. This is possible, since the true two-dimensional plasma has no such longitudinal quantum internal structure.

Collective excitations are completely described by the singular points of the density-density correlation functon, which is the system response function to an

external time and space dependent potential. This relationship is by now a part of the standard literature (20) (but for completeness it is summarized in Appendix D).

The calculation undertaken here is the determination of the plasma dispersion relation for a superlattice with electron plasma confined to regions of finite thickness. This introduces a non-classical element to the problem, since the confining subband electron wave functions should be explicitly taken into account. These subband wave functions are in general quite complex, since they self consistently take into account the band bending produced by migration of charge across the heterojunction, which in turn affects the electronic states and the consequent charge distribution which then redetermines the band bending itself. No attempt is made here to perform such a calculation, although such results are indeed important and are the subject of considerable research in superlattice theory. Suffice it to remark that when band bending is important the lower lying eigenfunctions are like those of an electron in a triangle well (see Fig. 5), a problem which has been much studied over the years in different contexts [e.g. particles in a gravitational field (21).]. Higher eigenstates of the bent potential exhibit tunneling into the neighboring superlattice layers (12) (see Fig. 3 and Fig. 4).

The calculation presented here avoids most of these complexities but still includes the finite thickness effect by use of the simplest wave functions which describe electron confinement to the plasma layer but which do not display tunneling. Physically the constraints imposed are those of low temperature and low carrier density, so that only the lowest subbands are occupied and band bending is minimal (the electron gas is confined in a sequence of square well potential as shown in Fig. 10. It proceeds by the determination of the particle-hole chanel of the two particle Green's Function $\Pi(x,x';\xi)$ in the Random Phase Approximation (RPA). There are some differences between the methods used here and those which are familiar from the plasmon theory of homogeneous systems, in that there is discreteness of propagators when superlattice subbands are included. This eventually leads in principle to the solution of a discrete matrix problem (18). The problem is examined here in the two subband limit and both the plasmon and resonant screened single particle excitations are studied.

Finally, it should be noted that the methods used here are capable of handling, within a superlattice tight binding model, any wave functions obtained by independent calculations. The importance of such sophistication expected to be considerable for the resonant screened single particle excitations, but less important for the plasmon modes.

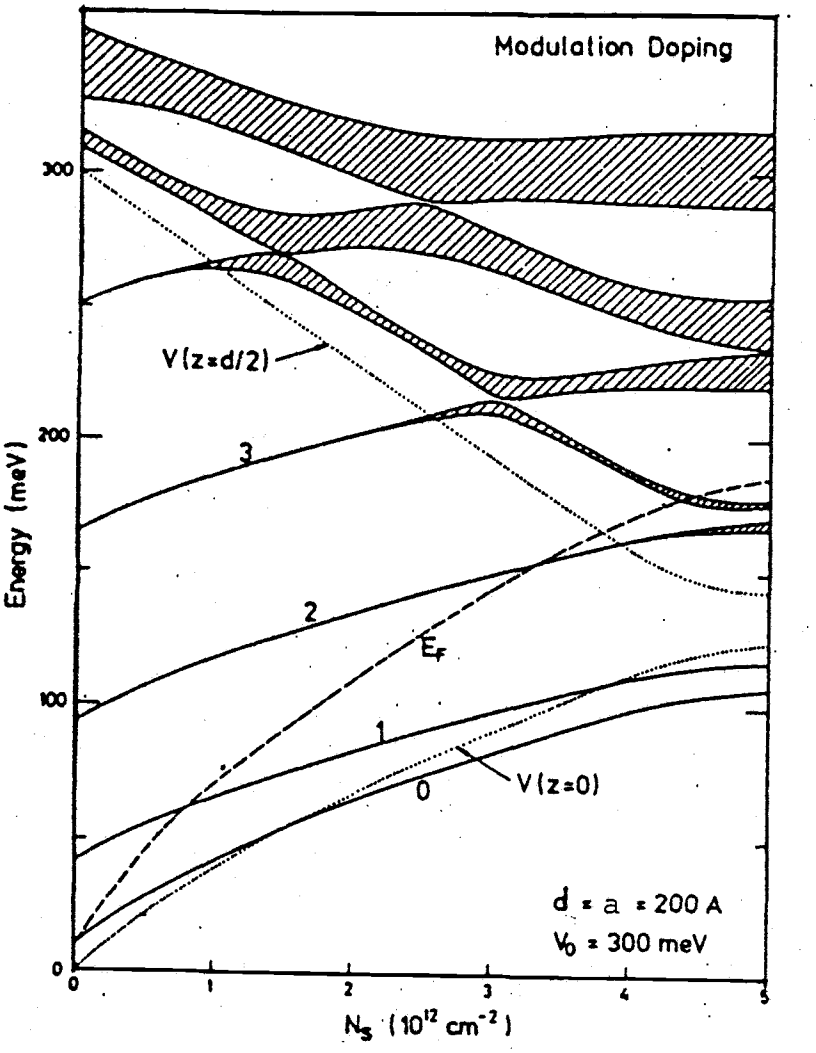

Fig.4.

Calculated energy spectra as a function of the electron concentration in the modulation doping case. The Fermi energy and the potential energy at z=0 and z=d/2 are also shown. The subband widths are described by hatches.

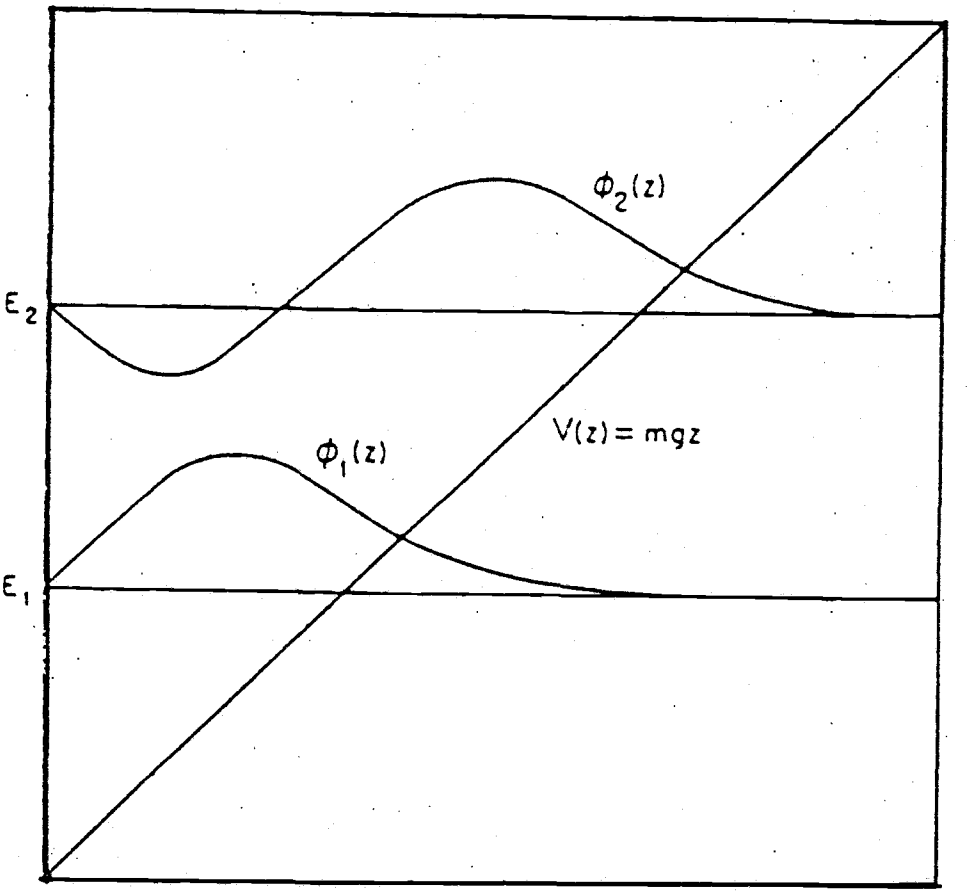

Fig.5.

General forms of the two lowest eigenfunctions for a particle moving in one direction in a uniform gravitational field(triangle potential well) above an impenetrable plane.

Chapter III

EXPERIMENTS

A. Introduction: Inelastic scattering of light

Probably the most suitable experiment for the investigation of collective excitation of electrons and holes of doped superlattices is first order (non-resonant) inelastic light scattering (8,23,24,25,27). In this case only the $\vec{A}\cdot\vec{A}$ part of the electron radiation interaction is retained for scattering by density fluctuations (collective modes) of electrons. The lowest order spectral differential cross section is formally given by (25)

$$\frac{d^2\sigma}{d\Omega d\omega_s} = \frac{e^4\omega_s V^2(\hat{\varepsilon}_I\cdot\hat{\varepsilon}_s)^2}{(4\pi\varepsilon_0)^2c^4m^2\omega_I}\sum_{i,f} n_i \left|\langle f\left|\rho^*(\vec{Q})\right|i\rangle\right|^2\delta(\omega-\omega_f+\omega_1) \tag{3.1}$$

where

$\omega_f = E_f + \Omega_s$

E_f : final electron state eigen energy

Ω_s : scattered photon frequency

$W_I = E_i + \Omega_I$

E_i : initial electron state eigen energy

Ω_I : incident photon frequency

V : the entire sample volume

m : effective mass of electrons

n_i : thermal distribution function of initial states

$|i\rangle$, $|f\rangle$: initial and final states of the many-electron system respectively

and $\rho(\vec{Q}) = \frac{1}{V}\sum_j \exp(-i\vec{Q}\cdot\vec{R}_j)$ is the $\vec{Q}$ Fourier component of the electron-density distribution, $\vec{Q} = (\vec{q}, q_z)$.

Since $\delta(\omega-\omega_f-\omega_I) = \frac{1}{2\pi}\int_{-\infty}^{\infty} dt\ e^{i\omega t}\ e^{-i\omega_f t}\ e^{i\omega_I t}$

and setting $h = 1$ (3.2)

$$\sum_{i,f} n_i \langle i|\rho(\vec{Q})|f\rangle\langle f|\rho^+(\vec{Q})|i\rangle\ \delta(\omega-\omega_f+\omega_I) \tag{3.3}$$

$$= \frac{1}{2\pi}\int dt \sum_{i,f} n_i \langle i|e^{i\omega_I t}\rho(\vec{Q})e^{-i\omega_f t}|f\rangle\langle f|\rho^+(\vec{Q})|i\rangle e^{i\omega t}$$

$$= \frac{1}{2\pi}\int dt \sum_{i,f} n_i \langle i|e^{iHt}\rho(\vec{Q})\ e^{-iHt}|f\rangle\langle f|\rho^+(\vec{Q})|i\rangle e^{i\omega t}$$

$$= \frac{1}{2\pi}\int dt \sum_{i,f} n_i \langle i|\rho(\vec{Q},t)|f\rangle\langle f|\rho^+(\vec{Q},0)|i\rangle e^{i\omega t}$$

$$= \frac{1}{2\pi}\int dt \sum_{i} n_i \langle i|\rho(\vec{Q},t)\rho^+(\vec{Q},0)|i\rangle e^{i\omega t}$$

$$= \frac{1}{2\pi}\int dt\ e^{i\omega t} \ll\rho(\vec{Q},t)\rho(\vec{Q},0)\gg = \ll\rho(\vec{Q})\rho^+(\vec{Q})\gg_\omega \tag{3.4}$$

where $\ll\rho(\vec{Q})\rho t(\vec{Q})\gg_\omega$ is the density-density correlation function with statistical average (temperature dependent). And hence

$$\frac{d^2\sigma}{d\Omega d\omega_s} = \frac{e^4\omega_s V^2(\hat{\varepsilon}_I\cdot\hat{\varepsilon}_s)^2}{(4\pi\varepsilon_0)^2c^4m^2\omega_I} < \hat{\rho}(\vec{Q})\ \hat{\rho}^+(\vec{Q})>_\omega \qquad (3.5)$$

The scattering cross section is therefore proportional to the frequency dependent density-density correlation function, which is usually evaluated by Green's Function methods. In particular the density-density correlation function is related to the time ordered density-density correlation (the polarization function)

$$\Pi(q,i\omega_n) = -\int_0^\beta d\tau\, e^{i\omega_n\tau} <T_\tau\ \rho(\vec{Q},\tau)\rho^+(\vec{Q},0)> \qquad (3.6)$$

where

$$\omega_n = \frac{2\pi n}{\beta}\ ,\ n = 0,\ \pm 1,\ \pm 2,\ \ldots\ldots\ ,\ \beta = \frac{1}{K_B T}$$

and τ is the coordinate of "time".

Through the fluctuation-dissipation theorem (28) (the general way of relating time ordered correlations to ordinary correlations),

$$\ll\rho(\vec{Q})\rho^+(\vec{Q})\gg_\omega = \frac{h}{\pi V}\,(n(\omega)+1)\ \operatorname{Im}_{\lim\delta\to 0^+}\ \Pi(\vec{Q},w+i\delta) \qquad (3.7)$$

where

$$n(\omega) = \frac{1}{e^{\beta\omega}+1}$$

Finally, the polarization Π is related to the dielectric response function $\varepsilon(Q,\ i\omega_n)$ by:

$$\frac{1}{\varepsilon(Q,i\omega_n)} = 1 - \frac{e^2}{\varepsilon_0 Q^2}\,\Pi(Q,i\omega_n) \qquad (3.8)$$

Thus we can conveniently write

$$\frac{d^2\sigma}{d\Omega d\omega s} = -\frac{e^2\omega_s \varepsilon_0 h V Q^2 (\hat{\varepsilon}_I \cdot \hat{\varepsilon}_s)^2}{(4\pi\varepsilon_0)^2 \Pi\, c^4\, m^2\, \omega_I}\,\{n(\omega)+1\}\,\mathrm{Im}\{\frac{1}{\varepsilon(\vec{Q},\omega)}\} \qquad (3.9)$$

and the cross section contains the properties of the many electron system through the form of the dielectric response function $\varepsilon(\vec{Q},\omega)$.

B. Experiment: Inelastic scattering of light

As mentioned before, the inelastic light scattering experiment is suited for the investigation of the collective excitation modes of periodically layered electrons of the superlattices since the layers are much thinner than optical wavelengths.

Recently, a determination of the plasma frequency dispersion in layered electron gases that occur in multiple GaAs-(Al_xGa_{1-x})As heterostructures (superlattice) has been reported (8). As discussed in chapter I, the dispersion relation observed in a layered electron system is expected to be different from that in 3-dimensional and 2-dimensional plasmas. The measurements, carried out by inelastic light scattering, show a linear dispersion over a wide range of in-plane (parallel to layers)

component of the wave vector. These results are in good qualitative agreement with the theory of the electrodynamics of layered electron plasmas (6,7). However there is a systematic discrepancy that has not been accounted for and does not allow the conclusion of quantitative agreement between theory and experiment. In reference (8) the possibility of inaccurately determined sample parameters is given as the source of the discrepancy. However, as discussed above the approach taken here is that the discrepancy is due to a more fundamental source.

GaAs-$(Al_xGa_{1-x})As$ multiple-quantum-well heterostructures were grown by Molecular Beam Epitaxy (MBE) on GaAs(001) substrates and modulation doped with Si donors. Their structure is shown schematically in Fig. 10. The electrons that vacate donor impurities in the $(Al_xGa_{1-x})As$ layers (of width a) are confined in the GaAs layers (of width d) where they occupy lower-energy states in the subbands. These charges constitute a layered electron gas with extremely high mobility carriers in excess of 5×10^4 cm^2/v sec. Results from two samples were reported. Sample 1 consists of 20 periods with d=262Å, a=628Å, total thickness L=1.78μm, x=0.20 and area density of impurity $n_s=7.3\times10^{11}cm^{-2}$. Sample 2 has 15 periods with d=245Å, a=582Å, L=1.24μm, x=0.11 and $n_s=5.5\times10^{11}cm^{-2}$.

Both samples introduce a low density electron gas in the GaAs layer, low enough for the simplifications used in the present theory to be applicable. The temperature was low enough (10°K) to justify the lowest subband occupying approximation used in chapter IV. Light scattering spectra were excited with an oxazine 750 dye laser operation between 7800Å and 7850Å. Backscattering like geometry in Fig. 6 was adopted to perform the experiment. θ and ϕ are taken as the angles between the normal and are chosen so that $\theta+\phi=90°$. The components of the scattering wave vector are given by

$$q = \frac{2\pi}{\lambda} (\sin\theta - \cos\theta) \quad \text{and}$$

$$q_z \approx \frac{4\pi}{\lambda} \cdot \eta\left(1 - \frac{1}{4\eta^2}\right)$$

This same notation is used in the theoretical results. here λ is the wavelength of the incident laser light and η corresponds to the wavelength dependent refractive index. By changing θ from 45° to 0°, q can be varied from a small value up to a maximum of $\sim 8\times10^{4}cm^{-1}$, which satisfies the condition $q(a+d)<1$ in samples 1 and 2.

For $\eta\approx3.6$, q_z has a large value of $\sim5.5\times10^{5}cm^{-1}$ and does not depend significantly on θ. By means of this geometry, the wave vector range $(q(a+d)<1)$ in which layering effects dominate can be probed. The

$(Al_xGa_{1-x})As$ layers are fortunately transparent to the laser photons. The absorption length α^{-1} in the GaAs layers is ~0.6μm, and consequently all the quantum wells are excitated. The condition $q_zL \gg 1$ holds, and the electrons should respond as if they were in an infinite array of planes.

Experimental light scattering spectra show several features. The peak energy positions of the collective states corresponding to sample 1 and sample 2 are plotted in Fig. 9 as a function of in plane wave vector (q). For θ larger than 35°, the scattered laser line dominates the scattered light and useful results can no longer be obtainable (see Fig. 8). The predicted plasma frequency based on DSQ (zero thickness of plama layers) is in C. G. S. units

$$\omega_p = \left[\frac{2\pi n_s e^2}{\varepsilon m^*} \frac{\sinh q\,a}{(\cosh qa - \cos q_z a)}\right] \qquad (3.10)$$

where a is the period of multilayers.

Normally the polarization selection rules allow the observation of intersubband transitions which are either pure spin-density (spin-flip) excitations of which scattering matrix elements is proportional to $(\varepsilon_I x \varepsilon_x)$ or pure charge-density (non-spin-flip) excitations which varies as $(\varepsilon_I \cdot \varepsilon_s)$ in first order (29,30). Therefore the former can then be observed in $z(y'x')\bar{z}$ spectra

and the latter in $z(x'x')\bar{z}$ spectra. Here z is the (001) propagation direction, normal to the layers, with x' and y' being (110) and $(1\bar{1}0)$ polarization directions in the two dimensional gas plane.

The energies of intersubband excitations are understood to be shifted from subband spacings by two effects associated with electron-electron interactions. One is an upward shift by resonant screening ($E_{\overline{01}}$) (see Fig. 7) and the other is a downward shift caused by the final state interaction between the ground state E_0 of hole and the first excited state of electron (31).

Final state interactions affect the single particle transition $E_0 \rightarrow E_1$ which is explored by the resonant Raman scattering experiment. The single particle scattering cross section dominates an experiment in which the incident and scattered polarizations are perpendicular. This type of polarization relationship arises due to a spin flip that takes place when the $E_0 \rightarrow E_1$ transition is made via spin-orbit split valence band intermediate states. It is not a first order effect.

The first order effect is due to charge density fluctuations through the $\vec{A}\cdot\vec{A}$ term in the Hamiltonian and gives a maximum contribution for incident and scattered polarizations which are parallel. Still, there is a second order contribution to the incident-scattered parallel

configuration which is also of single particle character but does not involve any spin flipping on the $E_0 \rightarrow E_1$ transition. It normally is small compared to first order effects, but can be enhanced when the resonance condition is met, i.e. $\omega_I \simeq 1.6$ eV (7750Å) for GaAs (the Oxazine 750 dye laser used in the experiment had wavelengths from 7800Å to 7850Å which is very near resonance). Thus there are two light scattering experiments depending on the relative directions of incident and scattered polarization.

The parallel configuration selects the collective mode behavior, i.e. plasmons and resonant screened shifted single particle excitations while the perpendicular configuration, near resonance, gives a substantial cross section for single particle transitions only.

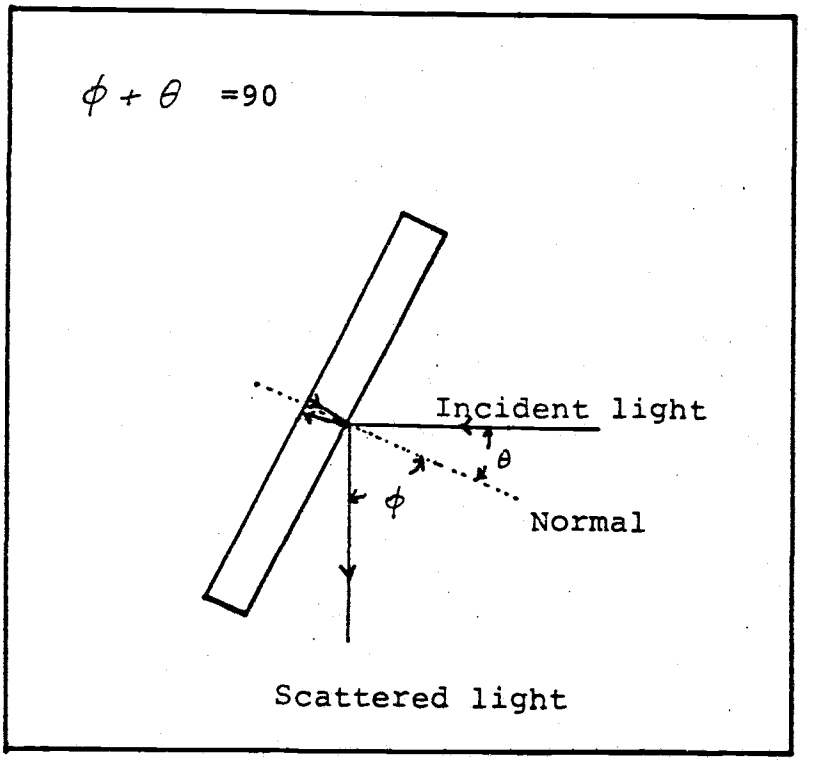

Fig. 6.

Scattering geometry adopted to perform the experiment.

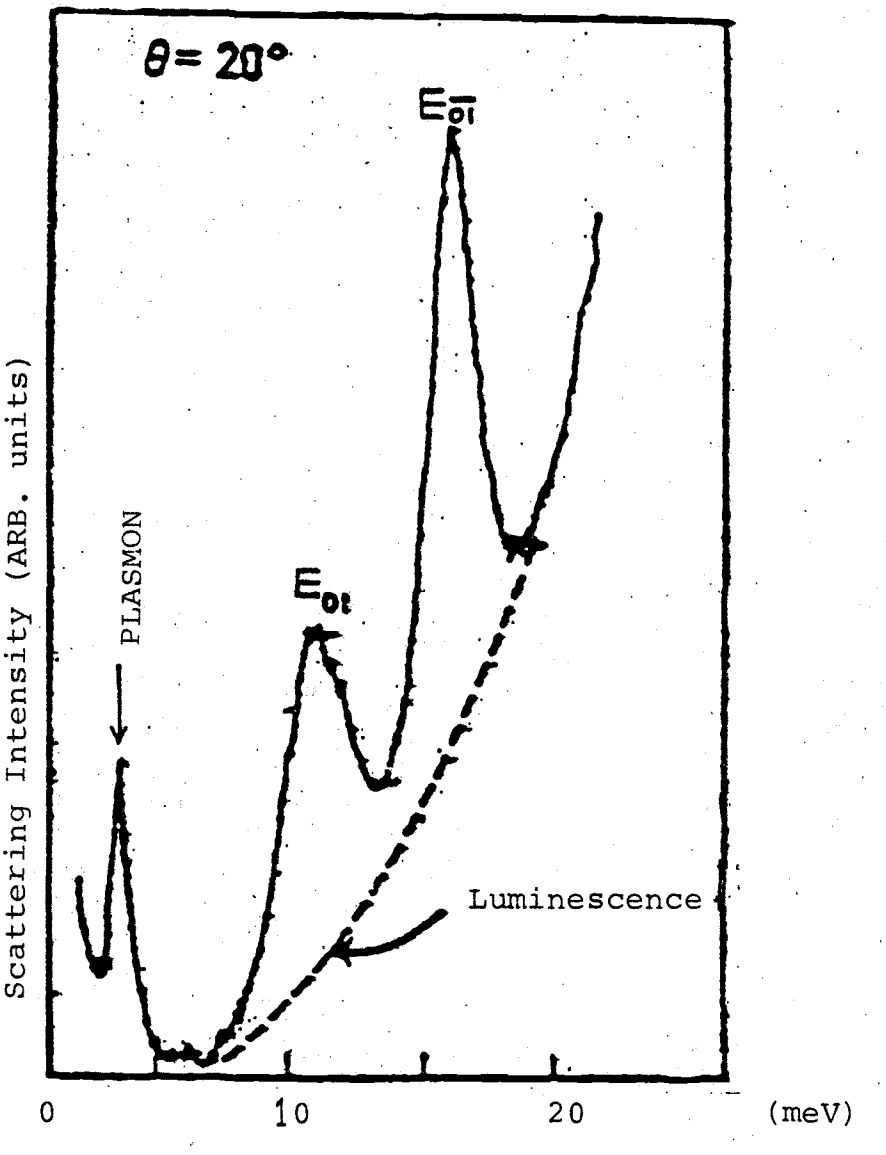

Fig. 7.

Typical light scattering spectra from Sample 1. The low-energy band is the layered electron gas plasmon.

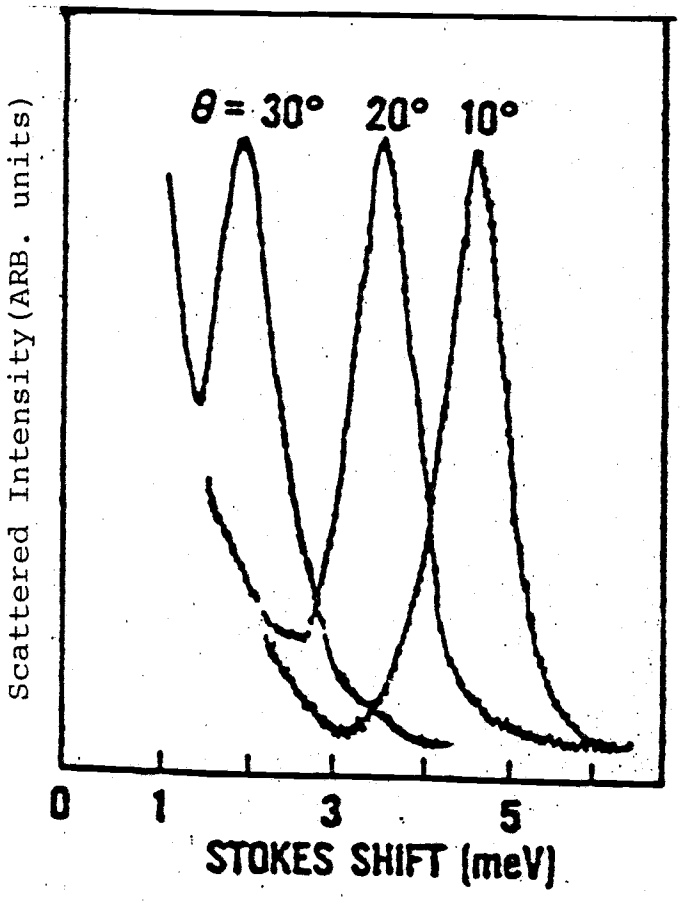

Fig. 8.

Plasmon lines of the layered electron gas for different angles θ . With increasing θ(decreasing q) the plasmon band shifts to lower energies.

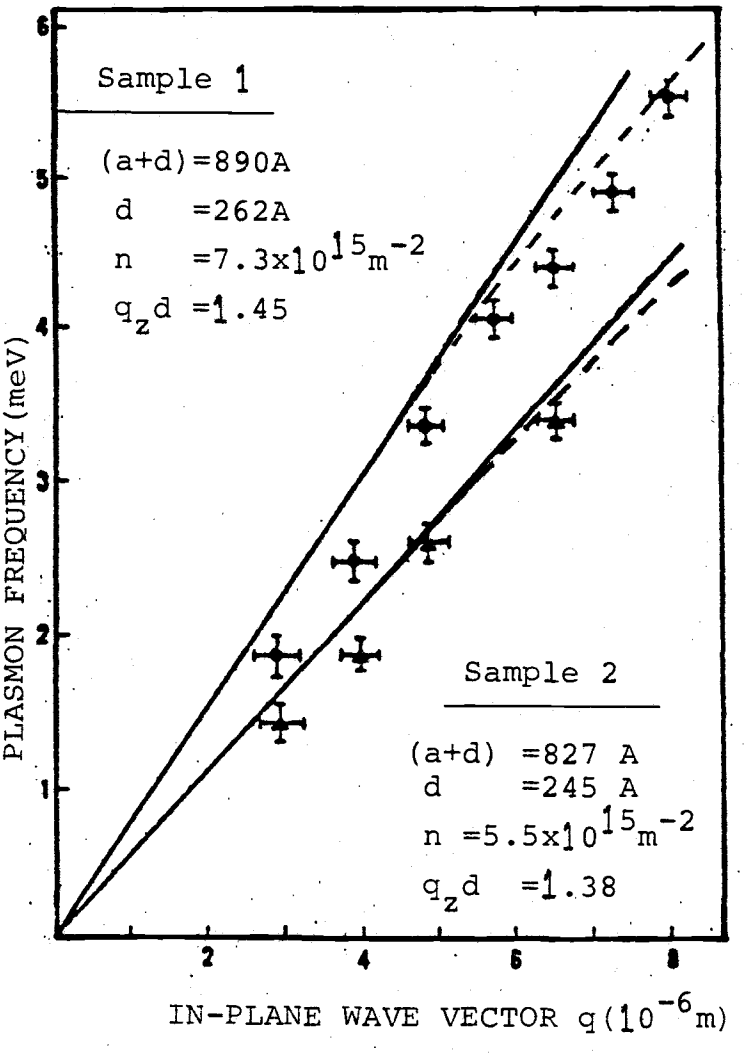

Fig. 9.

Dispersion relations of the plasma frequency of the layered electron gas in the two samples. The dotted lines are evaluations of Eq.(5.3)(Two dimensional electron gas layers model).

Chapter IV

RPA (RANDOM PHASE APPROXIMATION) THEORY OF COLLECTIVE ELECTRONIC EXCITATIONS IN THE TYPE I SUPERLATTICE

A. The GaAs-(Al_xGa_{1-x})As Superlattice Structure and Its Theoretical Model

The alternating expitaxial structure of GaAs and (Al_xGa_{1-x})As with donors such as Si is shown in Fig. 10. The addition of Al to the GaAs lattice causes only a relatively minor disturbance in the crystal structure because of its similar chemical valence and ionic size to Ga: yet it introduces an adequate amplitude of the superlattice potential in the conduction band, where the dynamics of electrons can be conveniently investigated. The schematic diagram in Fig. 10, which is the periodic system of square well potentials, is the model for this work. If the electron density is not too high, so that only the lowest subband is occupied by electrons, then at low temperature this simple model for a multilayer superlattice system is a reasonable approximation. From various experiments (i.e. mobility due to roughness scattering mechanism), it is believed that the boundary is atomically sharp. Under these conditions, the overlapping of electron wavefunctions from adjacent layers can be ignored.

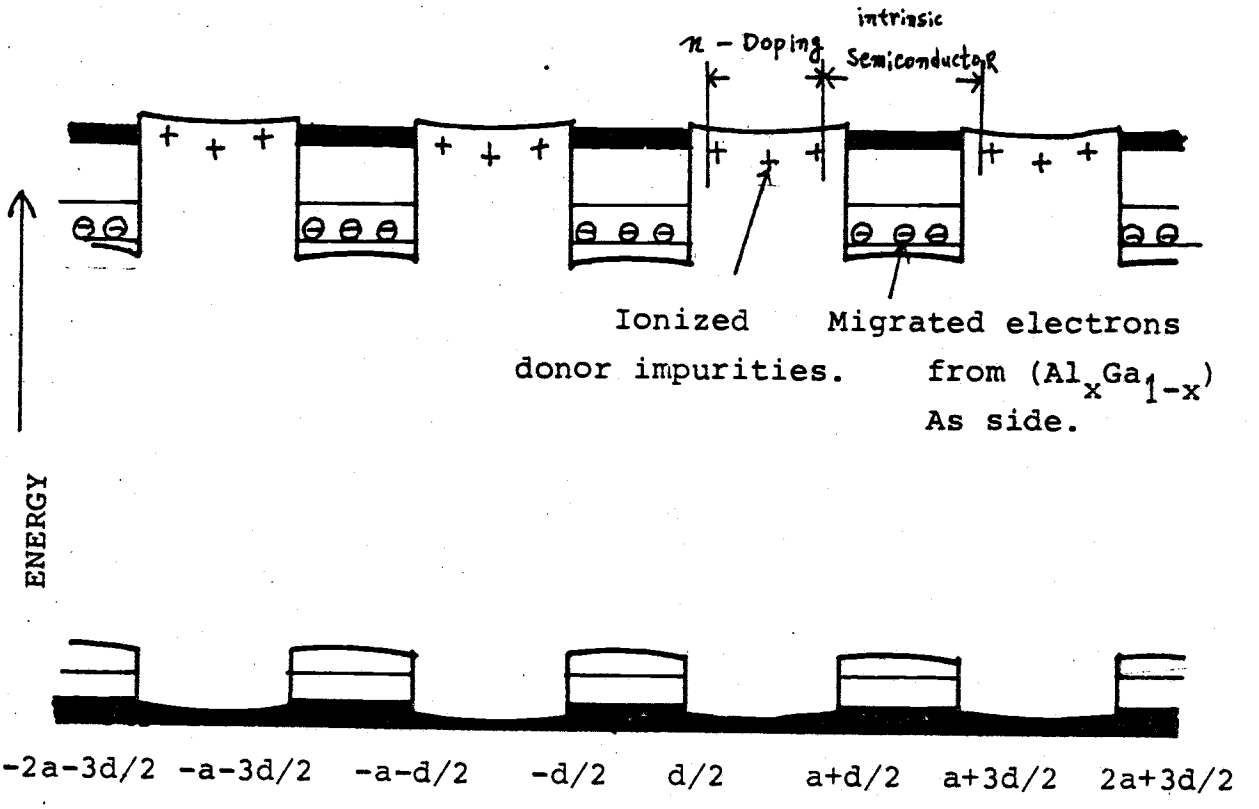

Fig. 10.

Doping of a compositional Superlattice.

B. Formalism

The dielectric response function is most simply calculated from the "time" ordered density-density correlation function (polarization) in the finite temperature Matsubara formalism. Defining the polarization

$$\Pi(x,x':\tau-\tau') = \langle T_\tau \{\psi^+(x,\tau)\psi(x,\tau)\psi^+(x',\tau')\psi(x',\tau')\}\rangle \quad (4.1)$$

where the brackets mean thermodynamic ensemble average and τ is the imaginary time as employed in the Matsubara formalism. Fourier expanding

$$\Pi(x,x':\xi_n) = \int_0^\beta d\tau\ \Pi(x,x':\tau,o)\ e^{i\xi_n\tau} \quad (4.2)$$

where τ is time analytically continued to the imaginary axis $-\beta < \tau < \beta$

$$\beta = 1/K_B T \ \underline{\text{and}}\ \xi_n = \frac{2n\pi}{\beta} \quad (3.3)$$

For the simpler type I superlattice structure $\pi(x,x':\xi_n)$ in the Random Phase Approximation (RPA) can be expressed as a sum of Feynman Diagrams.

$\Pi(x,x':\xi) =$

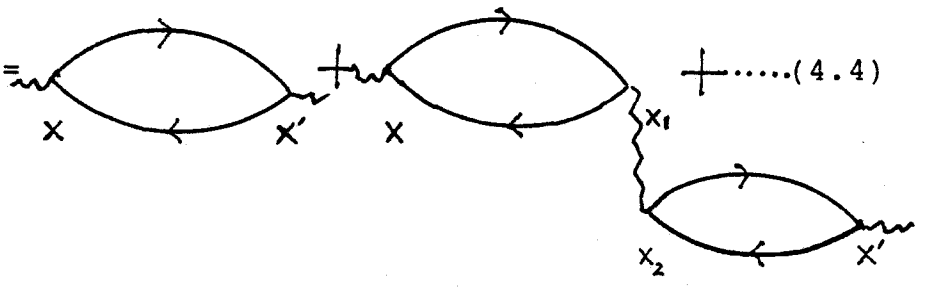

.....(4.4)

where each solid line is an electron (hole) propagator and each wiggling line is a coulomb interaction. The objective is to sum the contributions from all Feynman Diagrams using the propagators from some simpler exactly soluble problems. The coulomb interaction takes place between particles at different sites but at the same time. Each electron propagator has the form

$$G(x,x':\zeta_n) = \sum_j \frac{\phi_j(x)\ \phi_j^*(x')}{i\zeta_n - (E_j - \mu)} \qquad (4.5)$$

where

$$\zeta_n = \frac{(2n+1)}{\beta} \qquad n = 0, \pm 1, \ldots \text{ (for fermions)}$$

and μ is the chemical potential. The difference between electron and hole propagators is usually not an important distinction in finite temperature theory and $\phi_j(x)$ are the states appropriate for the exactly soluble problem and E_j are the corresponding eigenvalues. In the present case, the $\phi_j(x)$ are taken to be "superlattice tight binding" functions which can be of arbitrary complexity. This representation is appropriate since layer thickness is less than DeBroglie wavelengths. Their main feature is that they are made up from subband states in each superlattice layer. They will be written in greater detail

when the coulomb matrix elements are evaluated. Thus, the first term in this RPA series

$\Pi^{(o)}(x.x':\xi) \equiv$

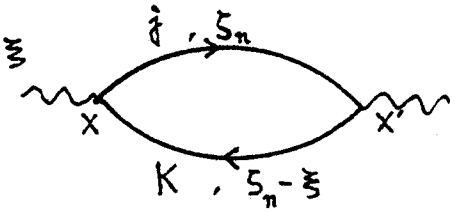

$$\equiv \sum_{\substack{j,k \\ \zeta_n}} \left[\frac{\phi_j(x)\phi_j^*(x')}{i\zeta_n-(E_j-\mu)}\right]\left[\frac{\phi_k^*(x)\phi_k(x')}{i(\zeta_n-\xi)-(E_k-\mu)}\right] \qquad (4.6)$$

(the spin coordinate has been suppressed).

and for the second term

$\Pi^{(1)}(x,x':\xi) \equiv$

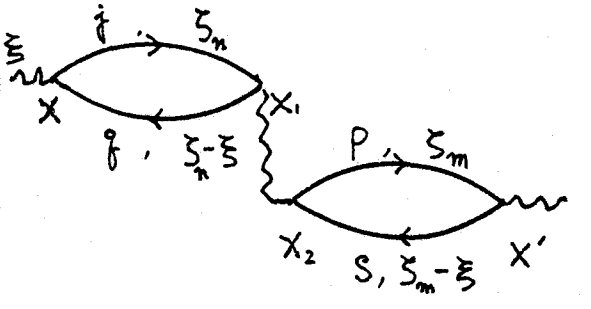

(4.7)

$$\equiv \sum_{\substack{j,p,q,s \\ \zeta_n \ \zeta_m}} \int dx_1 \int dx_2 \, \frac{\phi_j(x)\ \phi_j^*(x_1)}{i\zeta_n - (E_j - \mu)} \cdot \frac{\phi_p(x_1)\ \phi_p^*(x')}{i\zeta_m - (E_p - \mu)}$$

$$\frac{\phi_q(x)\ \phi_q^*(x_2)}{i(\zeta_n - \xi) - (E_q - \mu)} \cdot \frac{\phi_s(x_2)\ \phi_s^*(x')}{i(\zeta_m - \xi) - (E_s - \mu)} \ V(x_1 - x_2) \quad (4.8)$$

It is best to do the ζ_n, ζ_m .... sums first since this yields the most succinct form with which to work. Such sums [since $\zeta_n = \frac{(2n+1)\pi}{\beta}$] are easily done by contour integration. That is,

$$\sum_{\zeta_n} f(i\zeta_n) \to \frac{\beta}{2\pi i} \int_C \frac{1}{e^{\beta z}+1} f(z)\, dz \quad (4.9)$$

where the contour surrounds the poles of $(e^{\beta z}+1)^{-1}$ along the positive and negative imaginary axes

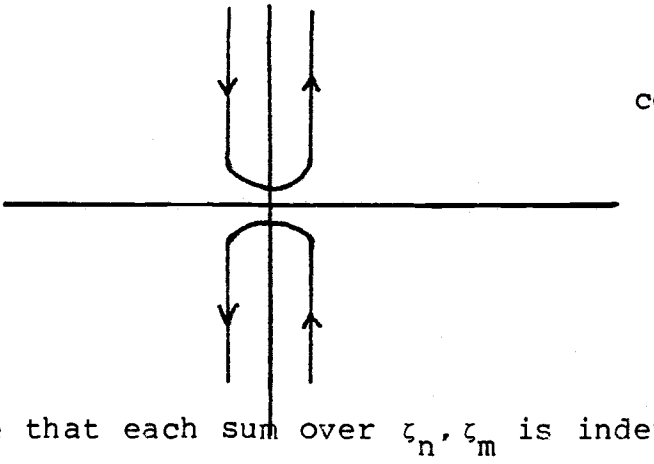

complex z plane

Note that each sum over ζ_n, ζ_m is independent. Deforming the contour and noting the poles of the integrand

$$\sum_{\zeta_n} \frac{1}{i\zeta_n - (E_j-\mu)} \cdot \frac{1}{i(\zeta_n-\xi) - (E_k-\mu)} =$$

$$\left[\frac{1}{e^{\beta(E_k-\mu)} + 1} - \frac{1}{e^{\beta(E_j-\mu)} + 1}\right] \frac{1}{i\xi + (E_k-E_j)} = \Pi_{kj}^{(0)} \quad (4.10)$$

Also writing the coulomb matrix elements as

$$V^{pqst} = \int dx_1 \int dx_2 \; \phi_p^*(\vec{x}_1)\phi_q(\vec{x}_2)\; V(x_1,x_2)\; \phi_s(\vec{x}_1)\; p_t^*(\vec{x}_2) \quad (4.11)$$

the terms in the series can be written

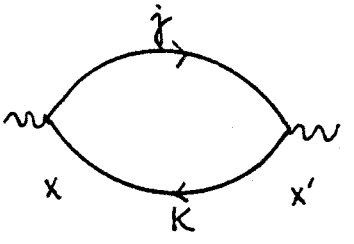

$$= \sum_{j,k} \Pi_{j,k}^{(0)}\; \phi_j(\vec{x})\; \phi_j^*(\vec{x}')\phi_k^*(\vec{x})\; \phi_k(\vec{x}')$$

$$= \sum_{j,k} \Pi_{j,k}^{(0)}\; J_{j,k}(\vec{x})\; J_{kj}(\vec{x}') \quad (4.12)$$

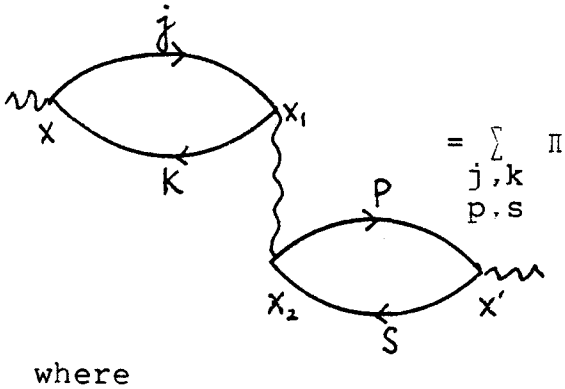

$$= \sum_{\substack{j,k \\ p,s}} \Pi_{jk}^{(0)}\; V_{jkps}\; \Pi_{ps}^{(0)}\; J_{jk}(\vec{x})\; J_{ps}(\vec{x}') \quad (4.13)$$

where

$$J_{jk}(x) = \phi_j(\vec{x})\; \phi_k^*(\vec{x}) \quad (4.14)$$

Since the indices all are repetitively paired we can write for simplicity

$$\Pi(x,x',\xi) = \sum_{\alpha\beta} \Pi_{\alpha}^{(0)} J_{\alpha}(x) \; [\delta_{\alpha\beta} + V_{\alpha\beta} \Pi_{\beta}^{(0)} + V_{\alpha\gamma} \Pi_{\gamma}^{(0)} V_{\gamma\beta} \Pi_{\beta}^{(0)} + \ldots.] \; J_{\beta}(x') \tag{4.15}$$

where, for example,

$$\Pi_{jk}^{(0)} \rightarrow \Pi_{\alpha}^{(0)}$$

$$V_{jk;ps} \rightarrow V_{\alpha;\beta} \tag{4.16}$$

The sum inside the bracket can be written as the matrix.

$$\chi_{\alpha\beta} = \delta_{\alpha\beta} + V_{\alpha\beta} \Pi_{\beta}^{(0)} + V_{\alpha\gamma} \Pi_{\gamma}^{(0)} V_{\gamma\beta} \Pi_{\beta}^{(0)} + \ldots.$$

$$= \delta_{\alpha\beta} + V_{\alpha\gamma} \Pi_{\gamma}^{(0)} \chi_{\gamma\beta} \tag{4.17}$$

$$[\delta_{\alpha\gamma} - V_{\alpha\gamma} \Pi_{\gamma}^{(0)}] \chi_{\gamma\beta} = \delta_{\alpha\beta} \tag{4.18}$$

so that

$$\Pi(x,x';\xi) = \sum_{\alpha} \Pi_{\alpha}^{(0)} J_{\alpha}(x) \chi_{\alpha\beta} J_{\beta}(x') \tag{4.19}$$

where

$$\chi_{\alpha\beta} = \delta_{\alpha\beta} [\delta_{\alpha\gamma} - V_{\alpha\gamma} \Pi_{\gamma}^{(0)}]^{-1} \tag{4.20}$$

and

$$[\delta_{\alpha\gamma} - V_{\alpha\gamma} \Pi_{\gamma}^{(0)}]^{-1} \tag{4.21}$$

is called the dielectric matrix.

To find collective modes, the zeros of the determinant of the dielectric matrix are located, i.e.,

$$\begin{vmatrix} 1 - V_{00}\Pi_0^{(0)} & V_{01}\Pi_1^{(0)} & V_{02}\Pi_2^{(0)} & \cdots \\ V_{10}\Pi_0^{(0)} & 1 - V_{11}\Pi_1^{(0)} & V_{12}\Pi_2^{(0)} & \cdots \\ V_{20}\Pi_0^{(0)} & V_{21}\Pi_1^{(0)} & 1 - V_{22}\Pi_2^{(0)} & \cdots \\ \vdots & \vdots & \vdots & \end{vmatrix} = 0 \qquad (4.22)$$

locates the collective modes. In the problem at hand the simplification is made such that only subband states $0 \to \nu$ ($\nu=0,1,2,\ldots$) are connected, where E_0 corresponds to the lowest subband energy. The subband separation is ~ 100°K. So at temperature 2 ~ 10°K and for low concentration such that ε_f < 10 meV, we can neglect the initial state occupancy of higher subbands. Thus the diagrams always look like

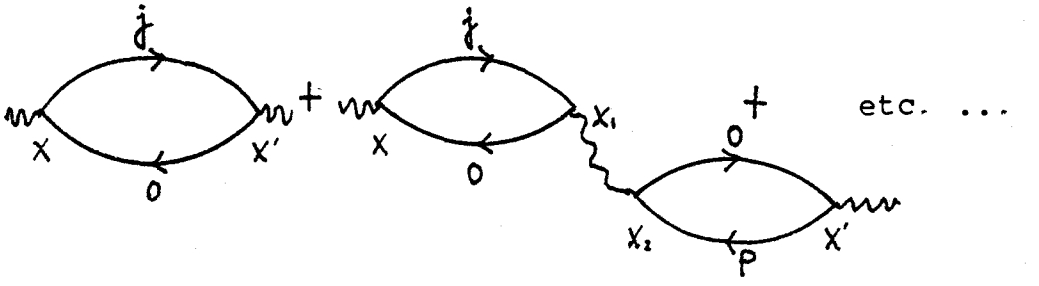

and the matrix elements are of the form

$$V_{jo,op} = \int \phi_p(x_2)\ \phi_j^*(x_1)\ V(x_1,x_2)\phi_0(x_1)\ \phi_0^*(x_2)\ dx_1\ dx_2$$

$$\equiv V_{\alpha\beta} \qquad \begin{matrix}\alpha = j,o \\ \beta = o,p\end{matrix} \qquad (4.23)$$

For classification we note that in this notation

$$V_{00} = \int dx_1\ dx_2\ \phi_0^*(x_1)\phi_0(x_1)\ V(x_1,x_2)\phi_0(x_2)\phi_0^*(x_2)$$

$$V_{11} = \int dx_1\ dx_2\ \phi_1^*(x_1)\phi_0(x_1)\ V(x_1,x_2)\phi_1(x_2)\phi_0^*(x_2)$$

$$V_{10} = \int dx_1\ dx_2\ \phi_1^*(x_1)\phi_0(x_1)\ V(x_1,x_2)\phi_0(x_2)\phi_0^*(x_2)$$

$$V_{01} = \int dx_1\ dx_2\ \phi_0^*(x_1)\phi_0(x_1)\ V(x_1,x_2)\phi_1(x_2)\phi_0^*(x_2) \qquad (4.24)$$

where the subscripts refer to the subband index.

C. Calculation of collective modes of layered electron gas in a Type I superlattice.

Electron motion parallel to the interface is considered free in the effective-mass approximation. For a given momentum parallel to the interface, the energy levels of the electrons in a square well potential of width d are quantized in the perpendicular direction to the layers (they are the same for all the layers). For our purpose, the envelope functions of an infinite square well potential of width d are used. (This is a reasonable approximation under the assumption of small band bending). If we neglect any image potential term in the interaction, the 3-dimensional coulomb interaction is as follows:

$$V(\vec{\rho}-\vec{\rho}',\ z-z') = \frac{e^2}{2\varepsilon}\frac{1}{[(x-x')^2+(y-y')^2+(z-z')^2]} \qquad \text{(M.K.S. Units)} \qquad (4.25)$$

where $\vec{\rho} = (x,y)$. (3.25)

If we use highly localized tight binding wavefunctions, then the ground state ($\nu=0$),

$$\phi_0(z) = \frac{1}{\sqrt{N}}\sqrt{\frac{2}{d}}\, e^{-i\vec{p}\vec{\rho}} \sum_m e^{-iq_z Z_m} \cos\frac{\pi}{d}[z-m(a+d)]$$

$$\cdot\{\theta[z-m(a+d)+d/2] - \theta[z-m(a+d)-d/2]\} \qquad (4.26)$$

setting $z-z_m=z-m(a+d)=\beta$, $z-z_n=z-n(a+d)=\beta'$,

then

$$\phi_0(z) = \frac{1}{\sqrt{N}} \frac{2}{\sqrt{d}} e^{-\vec{p}\vec{\rho}} \sum_m e^{-iq_z Z_m} \cos \frac{\pi}{d} \beta$$

$$\{\theta[\beta+d/2] - \theta[\beta-d/2]\} \qquad (4.27)$$

where $\vec{p} = (p_x, p_y)$

and $\nu \neq 0$ are the remaining eigenfunctions for particle in an infinite potential well. Performing the x and y integrations, we have

$$V_{\nu\nu'}(q) = \frac{e^2}{2\varepsilon} \int_{-\infty}^{\infty} dz \int_{-\infty}^{\infty} dz' \; \phi_\nu(z) \phi_0^*(z') \frac{e^{-q|z-z'|}}{q}$$

$$\phi_0^*(z) \phi_{\nu'}(z') \qquad (4.28)$$

where $\frac{e^2 e^{-q|z-z'|}}{2\varepsilon q}$ is the 2-dimensional Fourier transform of the coulomb potential (Appendix C). If we use the integral representation,

$$\frac{e^{-q|z-z'|}}{q} = \frac{1}{\pi} \int_{-\infty}^{\infty} ds \frac{e^{-is(z-z')}}{s^2+q^2} \qquad (4.29)$$

then

$$V_{00} = \frac{e^2}{2\pi\varepsilon} \int_{-\infty}^{\infty} ds \; \frac{1}{s^2+q^2} \int_{-d/2}^{d/2} \frac{1}{\sqrt{N}} \sqrt{\frac{2}{d}} e^{-is\beta} \sum_m e^{isZm} e^{-iq_z Zm}$$

$$\cos\left(\frac{\pi}{d}\beta\right) \frac{1}{\sqrt{N}} \sqrt{\frac{2}{d}} \sum_m e^{iq_z' Z_m} \cos\left(\frac{\pi}{d}\beta\right) d\beta \int_{-d/2}^{d/2} \frac{1}{\sqrt{N}} \sqrt{\frac{2}{d}}$$

$$e^{is\beta'} \sum_n e^{isZn} e^{iq_z'' Z_n} \cos\left(\frac{\pi}{d}\beta'\right) \frac{1}{\sqrt{N}} \sqrt{\frac{2}{d}} \sum_n e^{-iq_z''' Z_n}$$

$$\cos\left(\frac{\pi}{d}\beta'\right) d\beta'$$

$$= \frac{e^2}{2\pi\varepsilon} \frac{1}{N^2} \frac{4}{d^2} \int_{-\infty}^{\infty} ds \; \frac{1}{s^2+q^2} \sum_m e^{-i(s+q_z-q_z')Z_m} \int_{-d/2}^{d/2}$$

$$e^{-is\beta} \cos^2 \frac{\pi}{d}\beta \, d\beta \sum_n e^{i(s+q_z''-q_z''')Z_n} \int_{-d/2}^{d/2}$$

$$e^{is\beta'} \cos^2 \frac{\pi}{d}\beta' \, d\beta' \qquad (4.30)$$

But

$$\int_{-d/2}^{d/2} e^{-is\beta} \cos^2 \frac{\pi}{d}\beta \, d\beta = \frac{d}{4} \left\{ \frac{\sin\left[\left(s-\frac{2\pi}{d}\right)\frac{d}{2}\right]}{\left(s-\frac{2\pi}{d}\right)\frac{d}{2}} + \right.$$

$$\left. \frac{\sin\left[\left(s+\frac{2\pi}{d}\right)\frac{d}{2}\right]}{\left(s+\frac{2\pi}{d}\right)\frac{d}{2}} + 2 \frac{\sin\left(\frac{sd}{2}\right)}{\left(\frac{sd}{2}\right)} \right\} \qquad (4.31)$$

and

$$\sum_m e^{-i(s+q_z-q_z')Z_m} = N\delta(s+q_z+G) \quad ,$$

$$\sum_n e^{i(s+q_z''-q_z''')Z_n} = N\delta(s+q_z+G) \qquad (4.32)$$

Combining these results,

$$V_{00} = \frac{e^3}{4\varepsilon(a+d)} \sum_n \frac{1}{(q_z+G)^2+q^2} \left\{ \frac{\sin[(q_z+G-\frac{2\pi}{d})\frac{d}{2}]}{(q_z+G-\frac{2\pi}{d})\frac{d}{2}} + \right.$$

$$\left. \frac{\sin[(q_z+G+\frac{2\pi}{4})\frac{d}{2}]}{(q_z+G+\frac{2\pi}{d})\frac{d}{2}} + 2\,\frac{\sin[(q_z+G)\frac{d}{2}]}{(q_z+G)\frac{d}{2}} \right\}^2 \qquad (4.33)$$

where

$$G = \frac{2\pi}{(a+d)}\, n \qquad \text{and} \qquad n = 0, \pm 1, \pm 2, \ldots$$

and

$$V_{11} = \frac{e^2}{2\varepsilon} \int_{-\infty}^{\infty} dz \int_{-\infty}^{\infty} dz' \; \phi_1(z) \; \phi_0^*(z') \; \frac{e^{-q|z-z'|}}{q}$$

$$\phi_0^*(z)\phi_1(z') = \frac{e^2}{2\varepsilon} \frac{4}{N^2 d^2} \frac{1}{\pi} \int_{-\infty}^{\infty} ds \; \frac{1}{s^2+q^2} \int_{-d/2}^{d/2}$$

$$e^{-isZ_m} e^{-is\beta} \sum_m e^{-iq_z Z_m} \cos\left(\frac{\pi}{d}\beta\right) \sum_m e^{iq_z' Z_m}$$

$$\sin\left(\frac{2\pi}{d}\beta\right) d\beta \int_{-d/2}^{d/2} e^{isZn} e^{is\beta'} \sum_n e^{iq_z''}$$

$$\sin\left(\frac{2\pi}{d}\beta'\right) \sum_n e^{-iq_z''' Z_n} \cos\left(\frac{\pi}{d}\beta'\right) d\beta' \qquad (4.34)$$

But

$$\int_{-d/2}^{d/2} e^{-is\beta} \cos\frac{\pi}{d}\beta \sin\frac{2\pi}{d}\beta \, d\beta = \frac{1}{4i} \left\{ \frac{\sin(s-\frac{3\pi}{d})\frac{d}{2}}{(s-\frac{3\pi}{d})\frac{1}{2}} \right.$$

$$\left. - \frac{\sin(s+\frac{3\pi}{d})\frac{d}{2}}{(s+\frac{3\pi}{d})\frac{1}{2}} + \frac{\sin(s-\frac{\pi}{d})\frac{d}{2}}{(s-\frac{\pi}{d})\frac{1}{2}} - \frac{\sin(s+\frac{\pi}{d})\frac{d}{2}}{(s+\frac{\pi}{d})\frac{1}{2}} \right\} \qquad (4.35)$$

$$V_{11} = \frac{e^2}{4\varepsilon(a+d)} \sum_G \frac{1}{(q_z+G)^2+q^2} \left\{ \frac{\sin(q_z+G+\frac{3\pi}{d})\frac{d}{2}}{(q_z+G+\frac{3\pi}{d})\frac{d}{2}} \right.$$

$$\left. - \frac{\sin(q_z+G-\frac{3\pi}{d})\frac{d}{2}}{(q_z+G-\frac{3\pi}{d})\frac{d}{2}} + \frac{\sin(q_z+G+\frac{\pi}{d})\frac{d}{2}}{(q_z+G+\frac{\pi}{d})\frac{d}{2}} - \frac{\sin(q_z+G-\frac{\pi}{d})\frac{d}{2}}{(q_z+G-\frac{\pi}{d})\frac{d}{2}} \right\}^2 \tag{4.36}$$

$$V_{01} = V_{10}^* = \frac{e^2}{2\varepsilon} \int_{-\infty}^{\infty} dz \int_{-\infty}^{\infty} dz' \; \phi_0(z)\phi_1^*(z') \frac{e^{-q|z-z'|}}{q}$$

$$\phi_0^*(z) \; \phi_0(z') \tag{4.37}$$

$$= i \frac{-e^2}{4\varepsilon(a+d)} \sum_G \frac{1}{(q_z+G)^2+q^2} \left\{ \frac{\sin(q_z+G-\frac{2\pi}{d})\frac{d}{2}}{(q_z+G-\frac{2\pi}{d})\frac{d}{2}} \right.$$

$$\left. + \frac{\sin(q_z+G+\frac{2\pi}{d})\frac{d}{2}}{(q_z+G+\frac{2\pi}{d})\frac{d}{2}} + 2 \frac{\sin(q_z+G)\frac{d}{2}}{(q_z+G)\frac{d}{2}} \right\} \left\{ \frac{\sin(q_z+G-\frac{3\pi}{d})\frac{d}{2}}{(q_z+G-\frac{3\pi}{d})\frac{d}{2}} \right.$$

$$\left. - \frac{\sin(q_z+G+\frac{3\pi}{d})\frac{d}{2}}{(q_z+G+\frac{3\pi}{d})\frac{d}{2}} + \frac{\sin(q_z+G-\frac{\pi}{d})\frac{d}{2}}{(q_z+G-\frac{\pi}{d})\frac{d}{2}} - \frac{\sin(q_z+G+\frac{\pi}{d})\frac{d}{2}}{(q_z+G+\frac{\pi}{d})\frac{d}{2}} \right\} \tag{4.38}$$

We restrict our calculation to the two-subbands system so that collective intersubband excitations are given from the vanishing of the determinant [refer to Eq. (4.22)].

$$\begin{vmatrix} 1 - V_{00}\,\Pi_0^{(0)} & V_{01}\,\Pi_1^{(0)} \\ V_{10}\,\Pi_0^{(0)} & 1 - V_{11}\Pi_1^{(0)} \end{vmatrix} = 0 \qquad (4.39)$$

In considering the role of the polarization $\Pi_j^{(0)}$ for a system with finite plasma width, the contribution from subband formation must be considered. Recalling that sum over j and k are always required and that the states j,k have a two dimensional plane wave contribution parallel to the layers as well as the subband energy contribution perpendicular to the layers. We rewrite Eq. 4.10

$$\Pi_{kj}^{(0)} = \left\{ \frac{1}{e^{\beta(E_k-\mu)}+1} - \frac{1}{e^{\beta(E_j-\mu)}+1} \right\} \left(\frac{1}{i\xi+(E_k-E_j)} \right) \qquad (4.40)$$

In the choice of superlattice tight binding functions the effective mass of particles perpendicular to the stack is infinite due to the assumption of no tunneling between layers. Thus the terms involved are

$$\sum_{p} \frac{f(p+q,0)-f(p,0)}{\omega-(E_{p+q,0}-E_{p,0})/h} + \sum_{\nu,\rho} \frac{f(p+q,0)-f(p,\nu)}{\omega-(E_{p+q,0}-E_{p,\nu})/h}$$

$$+ \sum_{\nu,p} \frac{f(p+q,\nu)-f(p,0)}{\omega-(E_{p+q,\nu}-E_{p,0})/h} \qquad (4.41)$$

where

$$f(\nu) = \frac{1}{e^{(E_\nu-\mu)\beta}+1} \cdot E_{p,\nu} = \frac{h^2p^2}{2m^*} + E_\nu \cdot p^2 = p_x^2+p_y^2 \qquad (4.42)$$

If only the lowest subband $\nu=0$ is occupied, then the surviving terms are

$$\sum_{p} \frac{f(p+q,0)-f(p,0)}{\omega-(E_{p+q,0}-E_{p,0})/h} + \sum_{\nu,\rho} \left\{ \frac{f(p+q,0)}{\omega-(E_{p+q,0}-E_{p,\nu})/h} \right.$$

$$\left. - \frac{f(p,0)}{\omega-(E_{p+q,\nu}-E_{p,0})/h} \right\} \qquad (4.43)$$

The first term is called $\Pi_0^{(0)}(q,\omega)$ and the remaining term is therefore $\sum \Pi^{(0)}(q,\omega)$. The small q approximation for $\Pi_0^{(0)}(q,\omega)$is well known in the 2-dimensional RPA literature [see (5) for example or Appendix A].

$$\Pi_0^{(0)}(q,\omega) = \frac{n_s}{m^*}\frac{q^2}{\omega^2} \qquad (4.44)$$

The remaining term is also well approximated in the small q limit.

$$\Pi_\nu^{(0)}(q,\omega) = \sum_p \left\{ \frac{f(p+q,0)}{\omega-(E_0-E_\nu)/h} - \frac{f(p,0)}{\omega-(E_\nu-E_0)/h} \right\}$$

$$= \sum_p \left\{ \frac{f(p+q,0)}{\omega+\Delta_\nu} - \frac{f(p,0)}{\omega-\Delta_\nu} \right\} \qquad (4.45)$$

which for small q, becomes

$$\Pi_\nu^{(0)}(q,\omega) = \sum_p f(p,0)\left(\frac{-2\Delta_\nu}{\omega^2-\Delta_\nu^2}\right) \quad \text{Here } \Delta_\nu=(E_\nu-E_0)/h$$

$$= 2\, n_s \frac{\Delta_\nu}{\omega^2-\Delta_\nu^2} \quad \text{where } n_s \text{ is electronic area charge density.} \qquad (4.46)$$

For convenience we rewrite these as

$$\Pi_0^{(0)} = \frac{\tilde{\Pi}_0}{\omega^2} \quad , \quad \Pi_1^{(0)} = \frac{\tilde{\Pi}_1}{(\omega^2-\Delta_1^2)} \qquad (4.47)$$

where

$$\tilde{\Pi}_0 = \frac{n_s}{m^*} q^2 \quad \text{and} \quad \tilde{\Pi}_1 = 2\, n_s\, \Delta_1$$

setting $\Omega=\omega^2$, the collective frequencies are given by

$$\Omega = \frac{1}{2}\left\{ [V_{00}\tilde{\Pi}_0+(\Delta_1^2+ V_{11}\tilde{\Pi}_1)] \pm [V_{00}\tilde{\Pi}_0-(\Delta_1^2+V_{11}\tilde{\Pi}_1)] \right.$$

$$\left. \left(1 + \frac{4\left|V_{10}\right|^2 \tilde{\Pi}_0 \tilde{\Pi}_1}{[(V_{00}\tilde{\Pi}_0)-(\Delta_1^2+V_{11}\tilde{\Pi}_1)]^2}\right) \right\} \qquad (4.48)$$

Chapter V

RESULTS

A. Examination of limiting cases

The sums over reciprocal lattice vectors cannot be done in closed form except in the limiting case of thickness d=0. Then

$$\frac{\sin(q_z+G)\,\frac{d}{2}}{(q_z+G)\,\frac{d}{2}} \to 1 \tag{5.1}$$

and we can have following closed form for the collective modes

$$\Omega = \frac{n_s e^2}{\varepsilon\, m}\,\frac{q^2}{(a+d)}\sum_G \frac{1}{(q_z+G)^2+q^2} \tag{5.2}$$

after summing over G (Appendix E)

$$\omega = \left(\frac{n_s e^2}{2\varepsilon m}\, q\, \frac{\sinh q\, a}{(\cosh q\, a - \cos q_z a)}\right)^{1/2} \quad (C.G.S) \tag{5.3}$$

This is the hydrodynamic result of Fetter(7) and DSQ(6). This result is useful for discussing broad differences among the 2-dimensional, 3-dimensional bulk and superlattice systems.

a. First, consider the strong coupling case of vanishing separation between adjacent layers, long in-plane wavelengths, i.e. $qa \ll 1$ and $q_z \neq 0$. In this case, the contributions from induced electric fields in different layers tend to cancel (layering effects are dominant). Taking $qa \ll 1$ limit,

$$\omega_p = \left[\frac{n_s e^2}{2\varepsilon m}\,(1 - \cos q_z a)^{-1} a\right]^{1/2} q \qquad (5.4)$$

Thus all the modes for non zero q_z are "acoustic plasmas" with the characteristic superlattice linear dependence on q.

b. Secondly, consider the strong coupling case ($qa \ll 1$) in the limit of $q_z \to 0$ so that

$$\frac{\sinh q\,a}{\cosh q\,a - \cos q_z a} \simeq \frac{2}{qa} \qquad (5.5)$$

Therefore

$$\omega_p \simeq \left(\frac{n_s e^2}{\varepsilon m a}\right)^{1/2} = \left(\frac{n_v e^2}{\varepsilon m}\right)^{1/2} \quad \text{(M.K.S.)}$$

$$= \left(\frac{4\pi n_v e^2}{\varepsilon m}\right)^{1/2} \quad \text{(C.G.S.)} \qquad (5.6)$$

where $n_v = \frac{n_s}{a}$ · the effective 3-dimensional electron density of the superlattice.

This mode is the familiar 3-dimensional (bulk) plasmon dispersion which is independent of q (3.4).

c. Finally, consider the weakly coupling case of large separation between the adjacent layers ($qa \gg 1$) and small in plane wave vector component.

$$\frac{\sinh q\,a}{\cosh q\,a - \cos q_z a} \simeq 1 \qquad (5.7)$$

and

$$\omega_p \simeq \left(\frac{n_s e^2}{2\varepsilon m}\right)^{1/2} \sqrt{q} \qquad (5.8)$$

This mode has a pure two-dimensional behavior with the characteristic square-root wavevector dependence (i.e. each layer is independent) (5).

B. Two subband model calculations

The matrix elements are evaluated numerically because the sum over G cannot obviously be done in closed form except in the case d = 0. Calculation gives two eigenvalues for each value of q. One is the collective (plasmon) modes and the other a plasmon shifted intersubband excitation (also known as the depolarization field effect).

The off-diagonal contribution to the discrepancy between DSQ and our model is about the same as the diagonal term contribution (both are very small), so it should not be neglected. The results of calculation for the two different samples are in Table 1 and Table 2 and plotted in Fig. 11 and Fig. 12 (solid line). It should be noted that the two samples differ in both electron concentration and layer thickness. Also shown in these figures are Fetter and DSQ results (dashed curve) and results from the light scattering experiment (triangles and diamonds with error bars).

As mentioned in Chapter II, the DSQ calculation is systematically displaced from the experimental results for both samples. In contrast, the results from the two subband model are in excellent quantitative agreement with

experiment for both samples. Fig. 13 shows how the plasmon modes depend on the plasmon layer thickness for four different thicknesses and same concentration and whole periods (from the top, d=0, d=262Å, d=300Å and d=350Å). From the Fig. 13, we can see that the plasmon mode energies decrease systematically as the layer thickness increases. From the table 3, we can see that in terms of the degree of the thickness effect on the plasmon modes, what matters is the ratio of plasma layer thickness to the whole period.

In calculating the plasmon modes, the value of E_1-E_0 is required. The infinite square well wavefunctions are, by themselves, inadequate for such quantities because of band bending and final state interactions. We can instead regard the square well values as having been completely renormalized by the triangle well potential at the interface (32) and final state interactions (31) and use the values of E_1-E_0 obtained from light scattering experiment (8) for sample 1, i.e. E_1-E_0 = 11.3 meV. For sample 2, E_1-E_0 is obtained by scaling according to square well potential values. Ignoring n_s dependence of band bending and final state interactions is reasonable since the electron concentration is not too different in the two samples and E_1-E_0 varies slowly with the concentrations (12,31,33).

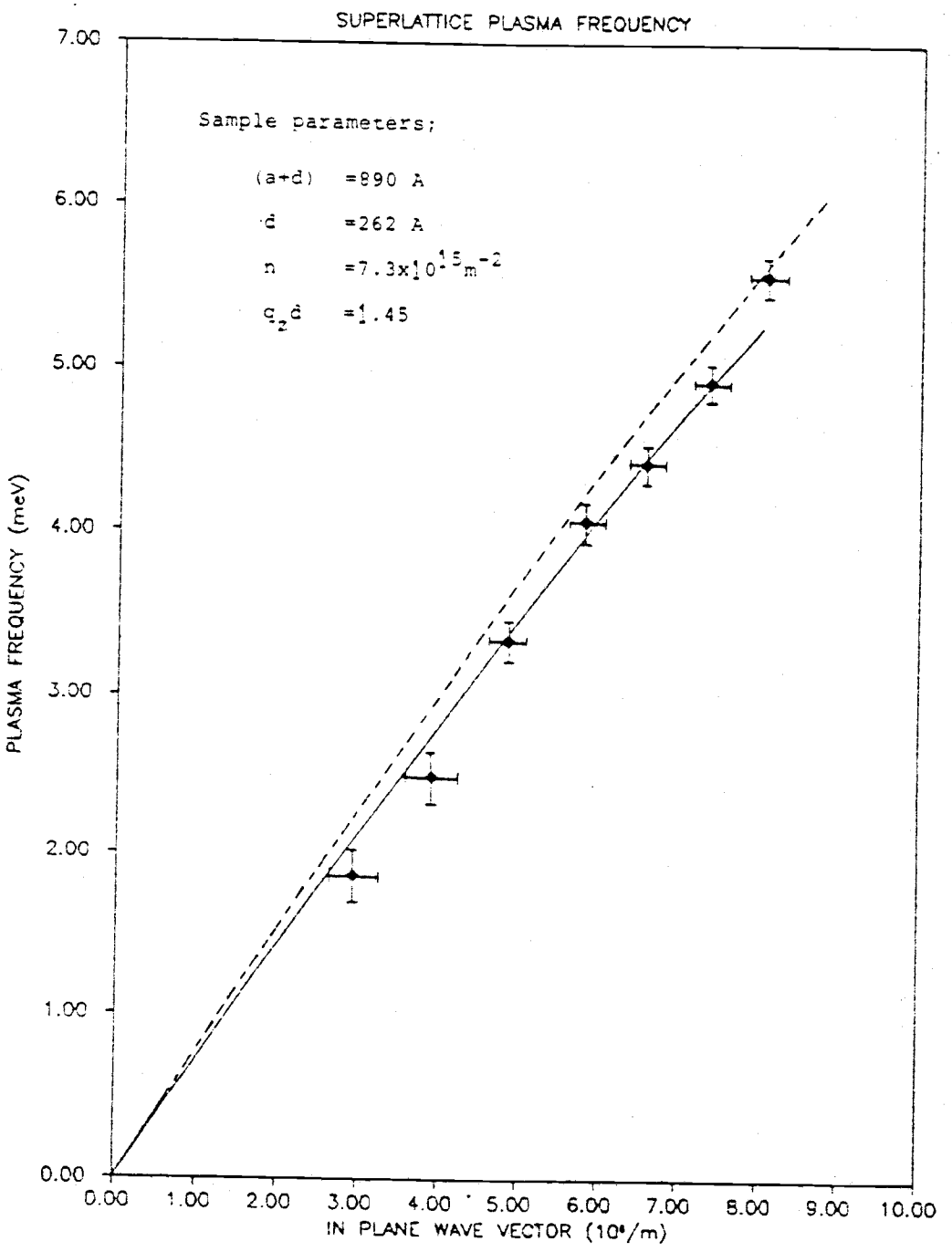

Fig. 11. Dispersion relations of the plasma frequency of the layered electron gas in the sample 1.

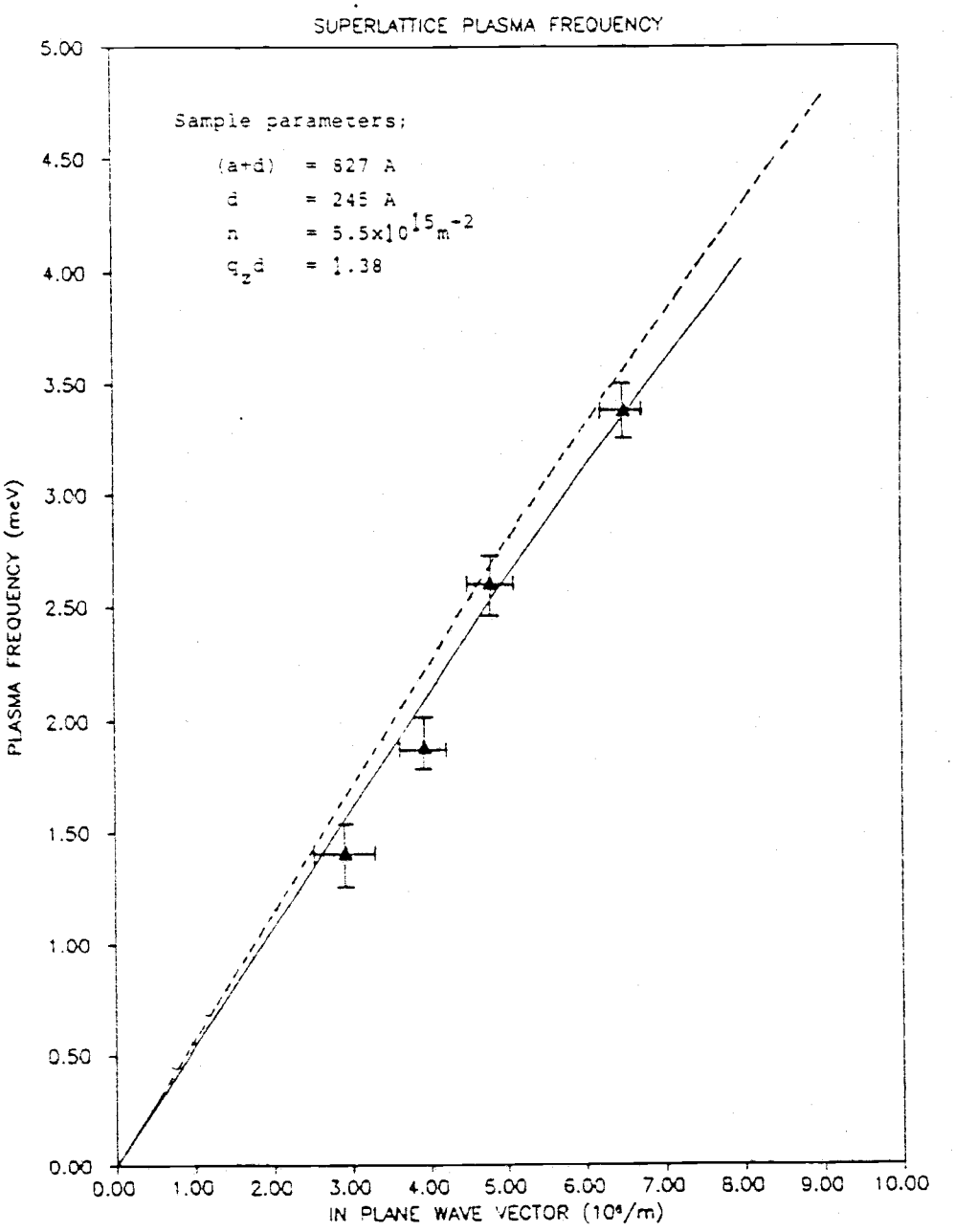

Fig. 12. Dispersion relations of the plasma frequency of the layered electron gas in the sample I.

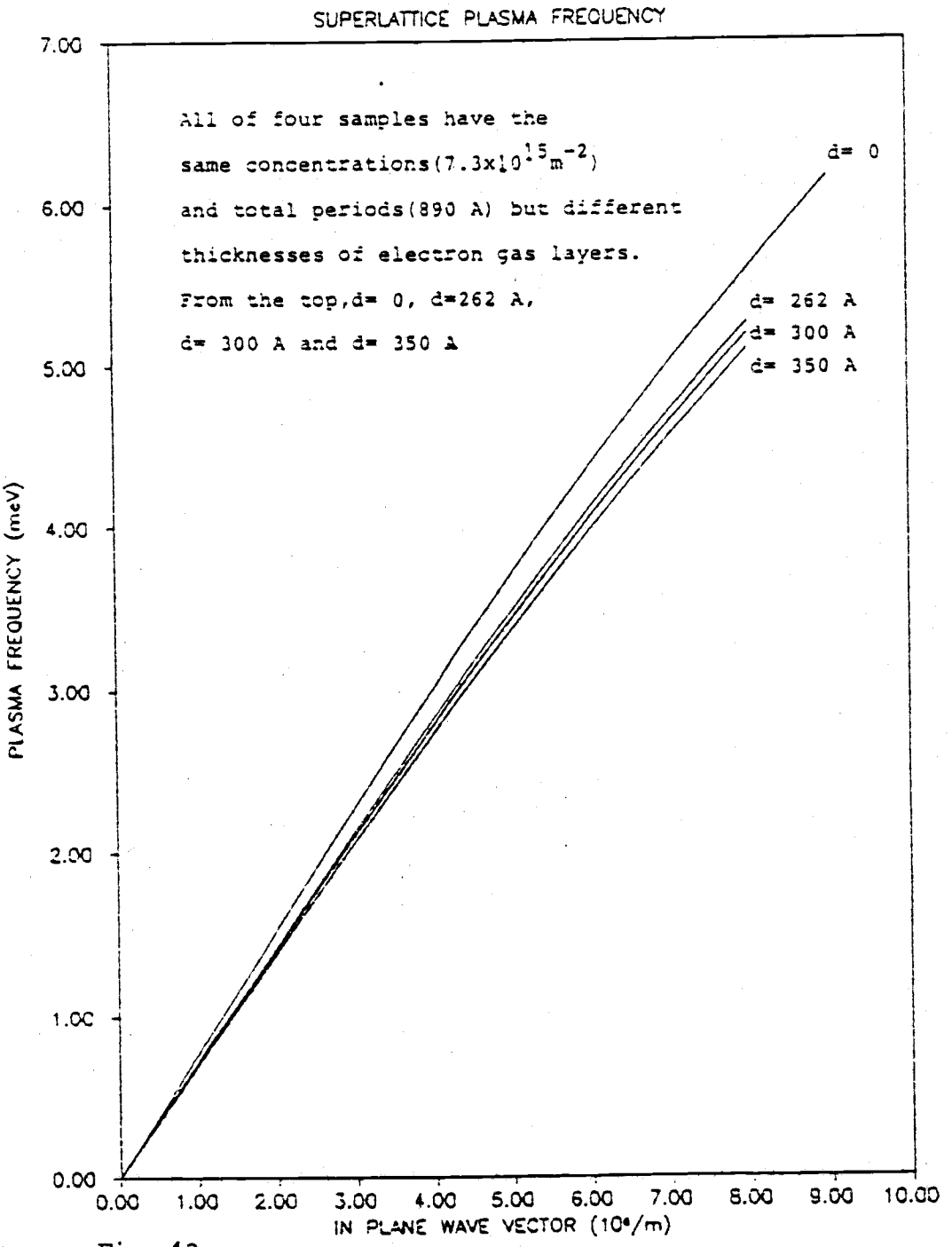

Fig. 13.
Dispersion relations of the plasma frequency of the layered electron gas for the three different samples.

TABLE I (Sample 1)

Area density = $7.3 \times 10^{15} m^{-2}$

Total period = $890 \times 10^{-10} m$

Layer thickness = $262 \times 10^{-10} m$

ΔE = 11.25 meV

q_z = $5.5 \times 10^{7} m^{-1}$

q_z ($\times 10^{6} m^{-1}$)	$\hbar\omega_p$ (meV)	$E_{\overline{01}}$ (meV)
0	0	21.48
.5	.36	21.48
1	.72	21.47
1.5	1.08	21.47
2	1.44	21.46
2.5	1.79	21.45
3	2.14	21.43
3.5	2.48	21.42
4	2.82	21.40
4.5	3.15	21.38
5	3.48	21.36
5.5	3.80	21.34
6	4.10	21.31
7	4.71	21.26
7.5	4.99	21.23
8	5.27	21.20

TABLE 2(Sample 2)

Area density $=5.5\times10^{15}m^{-2}$, Total period =827 A
Layer thickness = 245 A, ΔE =12.86 meV
q_z $=5.5\times10^{7}m^{-1}$

q_z $(\times10^{6}m^{-1})$	W_p (meV)	$E_{\overline{01}}$ (meV)
0	0	19.09
.5	.27	19.09
1	.54	19.09
1.5	.81	19.08
2	1.07	19.08
3	1.60	19.06
3.5	1.87	19.05
4	2.12	19.04
4.5	2.38	19.03
5	2.63	19.02
5.5	2.88	19.00
6	3.12	18.98
7	3.60	18.95
7.5	3.83	18.93
8	4.06	18.91

TABLE 3(Sample 3)

Area density $=4.2\times10^{15}m^{-2}$, Total period $=404\times10^{-10}m$,
Layer thickness $=204\times10^{-10}m$, ΔE =21.7 meV,
q_z $=7\times10^{7}m^{-1}$.

q_z $(\times10^{6}m^{-1})$	W_p (meV)	$E_{\overline{01}}$ (meV)
0	0	27.57
1	.23	27.57
2	.45	27.57
3	.68	27.56
4	.91	27.56
5	1.14	27.56
6	1.36	27.55
7	1.59	27.54
8	1.81	27.54

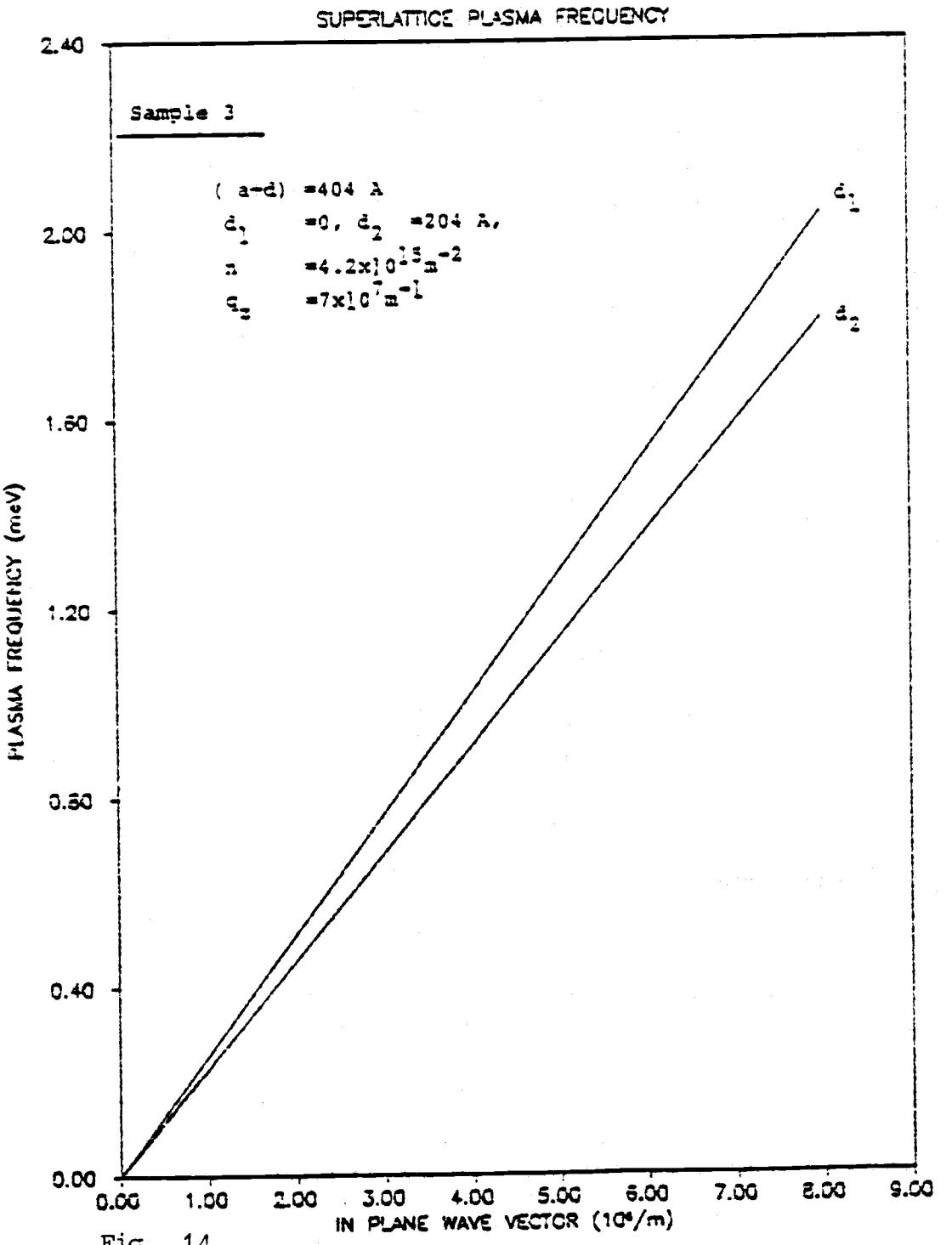

Fig. 14. Dispersion relations of the plasma frequency of the layered electron gas in the sample 3.

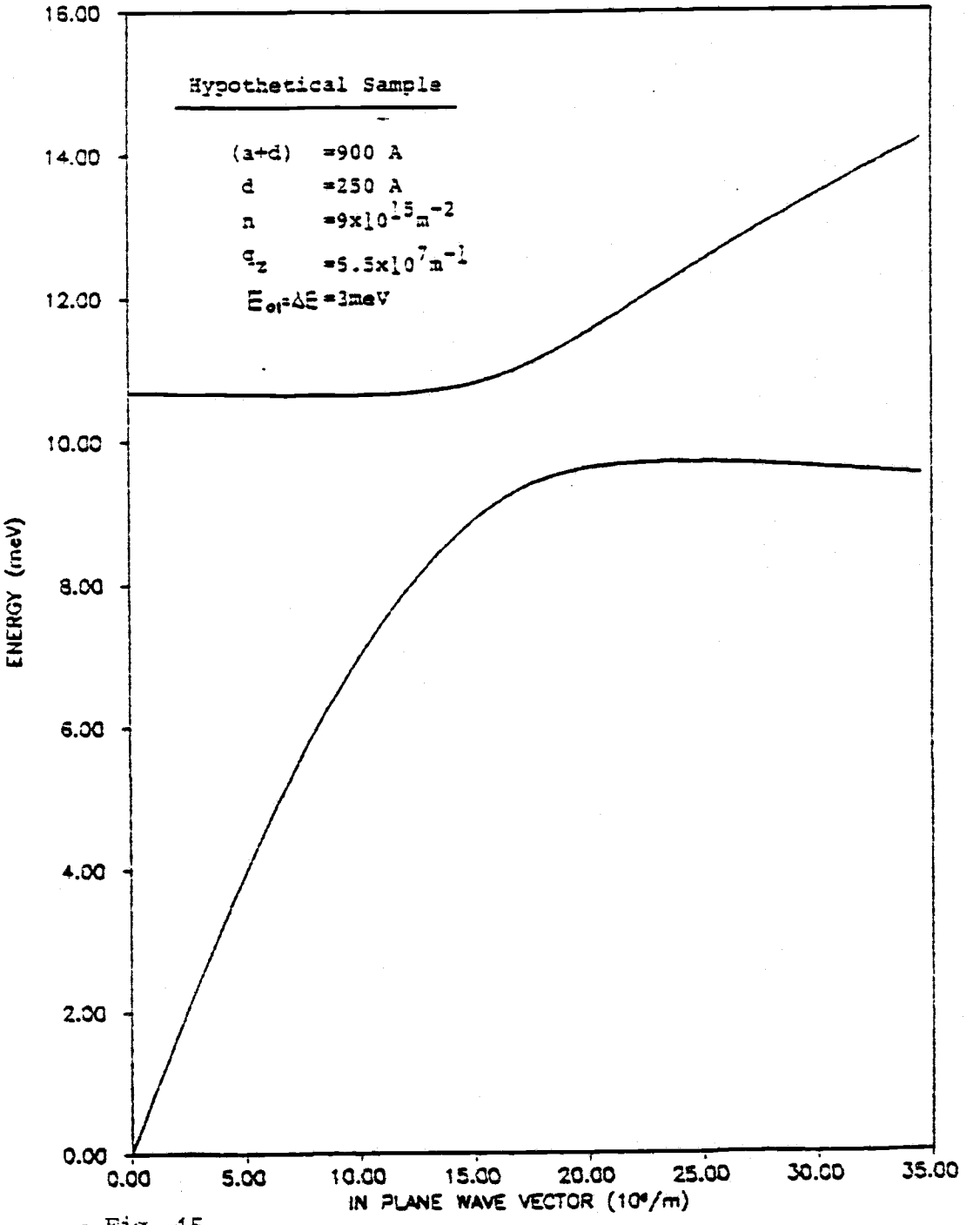

Fig. 15.
Dispersion relations of the plasma frequency of the layered electron gas in the hypothetical sample.

Chapter VI

CONCLUSIONS

There are a variety of optical experiments that have been mentioned earlier in conjunction with superlattice studies (13,14,15,16,17). Unfortunately most of these optical experiments are conducted at wavelengths that are too long to see individual superlattice layers except on average. Only the inelastic light scattering thus far gives any specific information about the internal superlattice struture (possibly inelastic electron scattering can be considered if very slow electrons can be produced). This does not mean that long wavelength transmission and absorption are not useful; it simply means that a detailed theory such as has been developed here is not required for average bulk optical properties of the superlattice.

Although the model which includes layer thickness gives only small changes from DSQ, they are just enough to remove the discrepancy between DSQ and the experiment. In reference (8) the possibility of inaccurately determined sample parameters is given as a possible source of the small discrepancies which cannot be totally discounted.

However, the approach taken here suggests that the discrepancy is due to a more fundamental source of finite thickness of the plasma layers.

The plasmon modes are affected by the off-diagonal terms which introduce dependence on $\Delta = (E_1-E_0)/h$. For sample 1 of reference (8) the experimental result for this quantity is used. For sample 2, in view of the fact that existing theory for these quantities is still inadequate, the expedient course of simply scaling the result of sample 1 for well width was done. It is believed that the problem of plasmon dispersion has been properly addressed in this work. There is little likelihood that using improved wave functions will be of much value for further study of this collective mode. However there still seems to be room for serious study of resonant screening effects which are both wavefunction sensitive and which depend on final state interactions.

The calculated value for the resonantly screened intersubband excitations which is shifted from subband spacing by one of two effects associated with electron-electron interaction known as resonant screening (depolarization field effect) is about 5 meV larger than the experimental result of reference (8). The reason for the

relatively large disagreement is not clear but the screening of the coulomb interaction by the polar lattice (resonant screening is itself screened by the polar lattice) improves the agreement by about 1 meV. This leaves the possibility that the matrix element dominant in determining this quantity is sensitive to the localized subband wave function and more accurate wave functions would improve the result. This hypothesis is yet to be tested since such wave functions are not yet routinely available. Since the longitudinal optical mode is ω_2=36.7 meV, there will be weak coupling between collective and phonon modes. But for other samples in which resonant screened intersubband excitations are close to phonon modes, we should account for the screening of the coulomb interaction by the polar lattice using the frequency dependent dielectric function

$$\varepsilon(\omega) = \varepsilon_\infty \frac{\omega_L^2 - \omega^2}{\omega_T^2 - \omega^2}$$

where for GaAs

$$\omega_T = 33.6 \text{ meV} \quad , \quad \omega_L = 36.7 \text{ meV}, \quad \varepsilon_\infty = 11$$

For the theoretical calculation presented here the envelope functions of an infinite square well potential of

small width (electron layers) were used. This is a reasonable approximation on the condition of low concentration of doping (10^{15} ~ 10^{16} m^{-2}), low temperature (~ 10°K) and small thickness of GaAs (electron gas) layers ($\leq$350Å). But if any of these conditions are not met (which means strong band bending), then one has to use more appropriate wavefunctions, e.g. Airy function in a triangle well potential. Finite band bending is thought to increase the overlap between envelope functions of the ground and first excited states,
so the present model calculation should give a somewhat smaller value for

$$L_{\alpha\beta} = \int_{-d/2}^{d/2} dz_1 \left(\int_{-d/2}^{d/2} dz_2 \, e^{-isz_2} \phi_0(z_2)\phi_2(z_2) \right) e^{-isz_1} \phi_0(z_1)\phi_\beta(z_1)$$

than realistic function might. This unfortunately only makes the present model less satisfactory. Further study, especially the role of final state interactions, is called for.

The effects of tunneling (overlap of electron wavefunctions from adjacent layers) have not been considered here. As we see from the Fig. 3 and Fig. 4, minibands are created due to the interaction between adjacent layers for

higher excited states. That's why it's wrong to extend our formalism and model to higher level system (larger matrix elements of V) for the case of high concentration, temperature and large thickness of electron gas layers (GaAs) even though they are correct to extend to higher level system under our approximation. For these states a localized model for confinement within layers is not applicable.

As a means to probe the plasma dispersion relationship even for large q, we can possibly use the inelastic electron scattering (inelastic light scattering is limited to small q). However there is likely to be great difficulty in preparing electron beams with energies in the meV range.

For Type II superlattice, unlike the Type I superlattice, every layer will absorb light. Therefore it will be very difficult to observe effects of plasmons such as is possible in the Type I superlattice system.

BIBLIOGRAPHY

(1) L. V. Keldysh. Sov. Phys. - Solid State 4. 1658-1659 (1962).

(2) G. H. Döhler, Phys. Status Solidi B52, 79-92 (1972).

(3) C. Kittel, Introduction to Solid State Physics, Wiley (New York), 289 (1976).

(4) J. D. Jackson, Classical Electrodynamics, Wiley (New York), 321 (1975).

(5) F. Sterm, Phys. Rev. Lett. 18, 546 (1967).

(6) S. Das Sarma, J. J. Quinn, Phys. Rev. B25, 7603 (1982).

(7) A. L. FEtter, Ann. Phys. (New York) 81, 367 (1973).

(8) Diego Olego, A. Pinczuk, A. C. Gossard, W. Wiegmann, Phys. Rev. B26, 7867 (1982).

(9) L. L. Chang, L. Esaki, Surf. Sci. 98, 70 (1980).

(10) L. Esaki, L. L. Chang, Thin Solid Films B26, 2851 (1976).

(11) I. B. Ortenburger, W. E. Rudge, IBM Internal Rep. RJ-1041, (1972).

(12) S. Mori, T. Ando, Surf. Sci. 98, 101 (1980).

(13) G. A. Sai-Halasz, L. L. Chang, J.-M. Welter, C.-A. Chang and L. Esaki, Solid State Comm. 27, 935 (1978).

(14) S. J. Allen, D. C. Tsui, Solid State Comm. 20, 425 (1976).

(15) J. C. Maan, M. Altarelli, H. Sigg, P. Wyder, L. L. Chang, L. Esaki, Surf. Sci. 113, 347 (1982).

(16) R. Al. Aggarwal, H. L. Störmer, A. C. Gossard, W. Wiegmann, Surf. Sci. 113, 89 (1982).

(17) P. Manuel, G. A. Sai-Halasz, L. L. Chang, Chin-An Chang, L. Esaki, Phys. Rev. Lett. 37, 1701 (1976).

(18) D. A. Dahl, L. J. Sham, Phys. Rev. B16, 651 (1977).

(19) S. Das Sarma, A. Madhukar, Phys. Rev. B23, 805 (1979).

(20) Fetter, Walechka, Quantum Theory of Many Particle Systems, McGraw-Hill (New York), (1971).

(21) P. W. Langhoff, American Journal of Phys. 39, 954 (1971).

(22) R. Dingle, A. C. Gossard, W. Wiegmann, Phys. Rev. Lett., 34, 1327 (1975).

(23) E. Burstein, A. Pinczuk, S. Buchner, Physics of Semiconductors 1978, edited by B. L. H. Wilson (The Institute of Physics, London 1979), p. 1231.

(24) A. Pinczuk, H. L. Störmer, R. Dingle, J. M. Worlock, W. Wiegmann, A. C. Gossard, Solid State Comm. 32, 1001 (1979).

(25) London, Scattering of Light by Crystals, John Wiley and Sons (New York), (1978).

(26) A. Pinczuk, J. M. Worlock, H. L. Störmer, R. Dingle, W. Wiegman, A. C. Gossard, Surf. Sci. 98, 126 (1980).

(27) A. Pinczuk, J. M. Worlock, H. L. Störmer, R. Dingle, W. Wiegmann, A. C. Gossard, Solid State Comm. 36, 43 (1980).

(28) D. N. Zubarev, Soviet Phys. Usp. 3, 320 (1960).

(29) D. C. Hamilton, A. L. McWhorter, paper D-4 in Proceedings of the 3rd Int. Conf. on Electronic Properties of Quasi Two Dimensional Systems, Lake Yamanaka, Japan, 1979.

(30) P. A. Wolff, Phys. Rev. 171, 436 (1968).

(31) S. Das Sarma, R. K. Kalia, M. Nakayama, J. J. Quinn, Phys. Rev. B24, 7181 (1981).

(32) F. Stern, W. E. Howard, Phys. Rev. 163, 816 (1967).

(33) S. Das Sarma, B. Vinter, Phys. Rev. B26, 960 (1982).

APPENDIX

APPENDIX A

Polarizability of a two-dimensional electron gas.

$$\chi(\vec{q},\omega) = \frac{e^2}{q^2\Omega} \cdot \lim_{\alpha\to 0} \sum \frac{f_0(E_{\vec{K}}) - f_0(E_{\vec{K}+\vec{q}})}{E_{\vec{K}+\vec{q}} - E_{\vec{K}} - \hbar\omega - i\hbar\alpha}$$

For second term, change variable $\vec{K}+\vec{q} \to \vec{K}$

$$= \lim_{\alpha\to 0} \sum_{K} \left[\frac{f_0(E_{\vec{K}})}{E_{\vec{K}+\vec{q}} - E_{\vec{K}} - \hbar\omega - i\hbar\alpha} - \frac{f_0(E_{\vec{K}})}{E_{\vec{K}} - E_{\vec{K}-\vec{q}} - \hbar\omega - i\hbar\alpha} \right]$$

For temperature $T=0$, $f_0(E_{\vec{K}}) = 1$

$$= \lim_{\alpha\to 0} \sum_{\vec{K}} \left[\frac{1}{E_{\vec{K}+\vec{q}} - E_{\vec{K}} - \hbar\omega - i\hbar\alpha} - \frac{1}{E_{\vec{K}} - E_{\vec{K}-\vec{q}} - \hbar\omega - i\hbar\alpha} \right]$$

$$\chi = (\chi_R' + i\chi_I') \frac{e^2}{q^2\Omega} = \chi_R + i\chi_I$$

$$\chi_I = \lim_{\alpha\to 0} \sum_{\vec{K}} \left[\frac{\hbar\alpha}{(E_{\vec{K}+\vec{q}} - E_{\vec{K}} - \hbar\omega)^2 + \hbar^2\alpha^2} - \frac{\hbar\alpha}{(E_{\vec{K}} - E_{\vec{K}-\vec{q}} - \hbar\omega)^2 + \hbar^2\alpha^2} \right]$$

$$= \sum_{\vec{K}} \left[\delta(E_{\vec{K}+\vec{q}} - E_{\vec{K}} - \hbar\omega) - \delta(E_{\vec{K}} - E_{\vec{K}-\vec{q}} - \hbar\omega) \right] = \text{Ⓐ} + \text{Ⓑ}$$

$$\text{Ⓐ} = \int K\,dK \int_0^{2\pi} \delta(\gamma q^2 + 2\gamma K q \cos\varphi - \hbar\omega)\, d\varphi$$

$$= \int K\,dK \int_0^{2\pi} \frac{\delta\left(\cos\varphi - \frac{(\gamma q^2 - \hbar\omega)}{2\gamma K q}\right)}{2\gamma K q}\, d\varphi$$

$$E_{\vec{K}+\vec{q}} = \frac{\hbar^2}{2m}(K^2 + q^2 + 2Kq\cos\varphi) = \gamma K^2 + \gamma q^2 + 2\gamma K q\cos\varphi,$$

$$\gamma = \frac{\hbar^2}{2m}$$

$$= \int K\,dK \int_0^{2\pi} \frac{\delta\left(\cos\varphi - \left(\frac{\gamma q^2 - \hbar\omega}{2\gamma K q}\right)\right)}{2\gamma K q(-\sin\varphi)}\, d(\cos\varphi)$$

$$= \int K\,dK \int_0^{2\pi} \frac{\delta\left(\cos\varphi - \frac{(\gamma q^2 - \hbar\omega)}{2\gamma K q}\right)}{2\gamma K q\ \sqrt{1-\cos^2\varphi}}\, d(\cos\varphi)$$

$$= \int K\cdot dK\ \frac{1}{2\gamma K q\ \sqrt{1-\left(\frac{\gamma q^2-\hbar\omega}{2\gamma K q}\right)^2}}$$

$$= \frac{1}{2\gamma q} \int \frac{K\,dK}{\sqrt{K^2 - \left(\frac{\gamma q^2 - \hbar\omega}{2\gamma q}\right)^2}}$$

Integration limits of k. From Dirac- Delta function,

$\gamma q^2 + 2\gamma K q\cos\varphi - \hbar\omega = 0$ (From Ⓐ)

$$-1 < \cos\varphi = \frac{(\hbar\omega - \gamma q^2)}{2\gamma K q} < 1 \quad \Rightarrow \quad \left|\frac{\hbar\omega - \gamma q^2}{2\gamma q}\right| < K$$

$-\gamma q^2 - 2\gamma q K\cos\varphi - \hbar\omega = 0$ (From Ⓑ)

$$-1 < \cos\varphi = \frac{\gamma q^2 + \hbar\omega}{2\gamma K q} < 1 \quad \Rightarrow \quad \left|\frac{\hbar\omega + \gamma q^2}{2\gamma q}\right| < K$$

For Ⓐ

$$K_{min} = \frac{\hbar\omega - \gamma q^2}{2\gamma q}, \qquad K_{max} = K_F.$$

For Ⓑ

$$K_{min} = \frac{\hbar\omega + \gamma q^2}{2\gamma q}, \qquad K_{max} = K_F.$$

Using (Dwight 261.01)

$$\textcircled{A} = \frac{1}{2\gamma q}\int_{k_{min}}^{K_F}\frac{K\,dK}{\sqrt{K^2-\left(\frac{\gamma q^2-\hbar\omega}{2\gamma q}\right)^2}}$$

$$= \frac{1}{2\gamma q}\left[\sqrt{K^2-\left(\frac{\gamma q^2-\hbar\omega}{2\gamma q}\right)^2}\right]_{\left(\frac{\hbar\omega-\gamma q^2}{2\gamma q}\right)}^{K_F}$$

$$= \frac{K_F}{2\gamma q}\sqrt{1-\left(\frac{\gamma q^2-\hbar\omega}{2\gamma q K_F}\right)^2}$$

Similarly,

$$\textcircled{B} = \int_{K_{min}}^{K_F} K\,dK\int_0^{2\pi} \delta\left(-\gamma q^2+2\gamma K q\cos\varphi-\hbar\omega\right)d\varphi$$

$$= \frac{K_F}{2\gamma q}\sqrt{1-\left(\frac{\gamma q^2+\hbar\omega}{2\gamma q K_F}\right)^2}$$

Therefore,
($\Omega = 1$),

$$\chi_I = \frac{e^2}{q^2}\left(\textcircled{A}-\textcircled{B}\right)$$

$$= \frac{e^2 K_F}{2\gamma q^3}\left[\left(1-\left(\frac{\gamma q^2-\hbar\omega}{2\gamma q K_F}\right)^2\right)^{1/2}-\left(1-\left(\frac{\gamma q^2+\hbar\omega}{2\gamma q K_F}\right)^2\right)^{1/2}\right]$$

$$z = \frac{q}{2K_F}, \quad u = \frac{\omega}{q v_F}$$

$$\chi_I = \frac{N e^2 K_F}{2\gamma q^3}\left[\left(1-(z-u)^2\right)^{1/2}-\left(1-(z+u)^2\right)^{1/2}\right]$$

Now, Let's calculate real part of

$$\chi_R' = \lim_{\alpha \to 0} \sum_{\vec{K}} \left[\frac{(E_{\vec{K}+\vec{q}} - E_{\vec{K}} - \hbar\omega)}{(E_{\vec{K}+\vec{q}} - E_{\vec{K}} - \hbar\omega)^2 + \hbar^2\vec{\alpha}^2} - \frac{(E_{\vec{K}} - E_{\vec{K}-\vec{q}} - \hbar\omega)}{(E_{\vec{K}} - E_{\vec{K}-\vec{q}} - \hbar\omega)^2 + \hbar^2\vec{\alpha}^2} \right] = \textcircled{A}' - \textcircled{B}'$$

$$\textcircled{A}' = \int_0^{K_F} K\,dK \int_0^{2\pi} \frac{d\varphi}{(\gamma q^2 + 2\gamma K q \cos\varphi - \hbar\omega)} = \int_0^{K_F} K\,dK \int_0^{2\pi} \frac{d\varphi}{(a + b\cos\varphi)}$$

$$a = \gamma q^2 - \hbar\omega \,, \quad b = 2\gamma K q$$

$$= \int_0^{K_F} K\,dK \left[\frac{2}{\sqrt{a^2 - b^2}} \tan^{-1} \frac{(a-b)\tan(\varphi/2)}{\sqrt{(a^2 - b^2)}} \right]_0^{2\pi} \qquad \text{(Dwight 446.)}$$

$$= 2\pi \int_0^{K_F} \frac{K\,dK}{\sqrt{(\gamma q^2 - \hbar\omega)^2 - (2\gamma K q)^2}}$$

Using Dwight (321.01)

$$= \frac{\pi}{\gamma q} \left[-\sqrt{\left(\frac{\gamma q^2 - \hbar\omega}{2\gamma q}\right)^2 - K^2} \right]_0^{K_F} = \frac{\pi K_F}{\gamma q} \left[-\sqrt{\left(\frac{\gamma q^2 - \hbar\omega}{2\gamma K_F q}\right)^2 - 1} + \sqrt{\left(\frac{\gamma q^2 - \hbar\omega}{2\gamma K_F q}\right)^2} \right]$$

$$\textcircled{B}' = \int_0^{K_F} K\,dK \int_0^{2\pi} \frac{d\varphi}{(-\gamma q^2 + 2\gamma q K \cos\varphi - \hbar\omega)} = \int_0^{K_F} K\,dK \int_0^{2\pi} \frac{d\varphi}{(a + b\cos\varphi)}$$

Where $\quad a = -(\gamma q^2 + \hbar\omega) \,, \quad b = 2\gamma K q \,.$

$$= \frac{\pi K_F}{\gamma q} \left[-\sqrt{\left(\frac{\gamma q^2 + \hbar\omega}{2\gamma q K_F}\right)^2 - 1} + \sqrt{\left(\frac{\gamma q^2 + \hbar\omega}{2\gamma q K_F}\right)^2} \right]$$

Setting,

$$\Omega = 1 \,,$$

$$\chi_R = \frac{e^2}{q^2}\chi_R'$$

$$= \frac{\pi e^2 K_F}{q^3 \gamma}\left\{\left[-\sqrt{\left(\frac{\gamma q^2-\hbar\omega}{2\gamma K_F q}\right)^2-1}+\sqrt{\left(\frac{\gamma q^2-\hbar\omega}{2\gamma q K_F}\right)^2}\right]\right.$$

$$\left.-\left[-\sqrt{\left(\frac{\gamma q^2+\hbar\omega}{2\gamma K_F q}\right)^2-1}-\sqrt{\left(\frac{\gamma q^2+\hbar\omega}{2\gamma K_F q}\right)^2}\right]\right\}$$

$$\sqrt{\left(\frac{\gamma q^2+\hbar\omega}{2\gamma q K_F}\right)^2}=\sqrt{(-1)\cdot\frac{\gamma q^2+\hbar\omega}{2\gamma K_F q}}=-\frac{(\gamma q^2+\hbar\omega)}{2\gamma q K_F}$$

$$\chi_R = \frac{N\pi e^2 K_F}{\gamma q^2}\left\{\left[-\sqrt{\left(\frac{\gamma q^2-\hbar\omega}{2\gamma q K_F}\right)^2-1}-\left(-\sqrt{(-1)\frac{\gamma q^2+\hbar\omega}{2\gamma q K_F}-1}\right)\right]+\frac{2\gamma q^2}{2\gamma q K_F}\right\}$$

$$= \frac{N\pi e^2 K_F}{\gamma q^2}\left\{\left[-\sqrt{(z-u)^2-1}-\sqrt{(-1)^2(z+u)^2-1}\right]+2z\right\}.$$

MAXWELL EQUATIONS

$$\vec{\nabla} \times \vec{E} = -\frac{1}{c}\frac{\partial \vec{B}}{\partial t}$$

$$\vec{\nabla} \times \vec{B} = \frac{4\pi}{c}\vec{J} + \frac{1}{c}\frac{\partial \vec{D}}{\partial t}$$

Combining these two equations,

$$\vec{\nabla} \times (\vec{\nabla} \times \vec{E}) = -\frac{1}{c}\frac{\partial}{\partial t}(\vec{\nabla} \times \vec{B}) = -\frac{1}{c}\frac{\partial}{\partial t}\left(\frac{4\pi}{c}\cdot\vec{J} + \frac{1}{c}\frac{\partial \vec{D}}{\partial t}\right)$$

Take $\vec{J} = 0$ (No real currents)

E(r,t) and B(r.t) be the electric field and magnetic field associated with the plasma oscillations.

$$\vec{\nabla} \times (\vec{\nabla} \times \vec{E}) = -\frac{1}{c^2}\frac{\partial^2 \vec{D}}{\partial t^2}$$

$$\vec{\nabla}(\vec{\nabla}\cdot\vec{E}) - \nabla^2\vec{E} + \frac{1}{c^2}\frac{\partial^2 \vec{D}}{\partial t^2} = 0$$

$\vec{\nabla}\cdot\vec{E} = \rho$ is not constant (is a function of position).

In matter,

Polarization charge is preserved (at least).

$$\vec{D} = (1 + 4\pi\chi')\vec{E}$$

$P_i = \chi_{ij} E_j$ (Linear response)

Assuming

$$\chi' = \chi_B + \chi\,\delta(z)$$

χ_B ; background dielectric susceptibility.

$\vec{E}$ and $\vec{P} \sim e^{i\omega t}$

$$\vec{\nabla}\cdot(\vec{\nabla}\cdot\vec{E}) - \nabla^2\vec{E} - \frac{\omega^2}{c^2}\vec{D} = 0$$

$$\vec{\nabla}\cdot(\vec{\nabla}\cdot\vec{E}) - \nabla^2\vec{E} - \frac{\omega^2}{c^2}\vec{E} = \{4\pi\chi_B\vec{E} + 4\pi\chi\delta(\vec{z})\vec{E}\}\frac{\omega^2}{c^2}$$

Equation has three component equation .

$$\frac{\partial}{\partial x}\left(\frac{\partial}{\partial x}E_x + \frac{\partial}{\partial y}E_y + \frac{\partial}{\partial z}E_z\right) - \left(\frac{\partial^2}{\partial x^2} + \frac{\partial^2}{\partial y^2} + \frac{\partial^2}{\partial z^2}\right)E_x - \frac{\omega^2}{c^2}\left(1 + 4\pi\chi_B + 4\pi\chi_{xx}\delta(z)\right)E_x = 0$$

$$\frac{\partial}{\partial y}\left(\frac{\partial}{\partial x}E_x + \frac{\partial}{\partial y}E_y + \frac{\partial}{\partial z}E_z\right) - \left(\frac{\partial^2}{\partial x^2} + \frac{\partial^2}{\partial y^2} + \frac{\partial^2}{\partial z^2}\right)E_y - \frac{\omega^2}{c^2}\left(1 + 4\pi\chi_B + 4\pi\chi_{yy}\delta(z)\right)E_y = 0$$

$$\frac{\partial}{\partial z}\left(\frac{\partial}{\partial x}E_x + \frac{\partial}{\partial y}E_y + \frac{\partial}{\partial z}E_z\right) - \left(\frac{\partial^2}{\partial x^2} + \frac{\partial^2}{\partial y^2} + \frac{\partial^2}{\partial z^2}\right)E_z - \frac{\omega^2}{c^2}\left(1 + 4\pi\chi_B + 4\pi\chi_{zz}\delta(z)\right)E_z = 0$$

Set, $1 + 4\pi\chi_B = K_B$; the dielectric constant of the background.

Fourier Transform,

$$E_j = \int E_j(p, s; \omega)\,\frac{e^{-i\vec{p}\cdot\vec{x}}}{(2\pi)^2}\,\frac{e^{-isz}}{(2\pi)}\,d\vec{p}\,ds\,\frac{e^{-i\omega t}}{(2\pi)}\,dt$$

Where $\vec{p}\cdot\vec{x} = p_x x + p_y y$

$$i p_x\, i p_y\, E_y(\vec{p}, s) + i p_x\, i s\, E_z(\vec{p}, s) + p_y^2 E_x(\vec{p}, s) + s^2 E_x(\vec{p}, s) - \frac{\omega^2}{c^2}K_B E_x(\vec{p}, s) - 4\pi\chi_{xx}\frac{\omega^2}{c^2}E_x(z=0) = 0$$

$$-p_x p_y E_x(\vec{p}, s) - p_y s E_z(\vec{p}, s) + p_x^2 E_y(\vec{p}, s) + s^2 E_y(\vec{p}, s) - \frac{\omega^2}{c^2}K_B E_y(\vec{p}, s) - 4\pi\chi_{yy}\frac{\omega^2}{c^2}E_y(z=0) = 0$$

$$-s p_x E_x - s p_y E_y + p_x^2 E_z + p_y^2 E_z - \frac{\omega^2}{c^2}K_B E_z - \frac{\omega^2}{c^2}4\pi\chi E_z(z=0) = 0$$

We can choose $P_x = 0$ without loss of generality

$$\left(P_y^2 + S^2 - \frac{\omega^2}{c^2} K_B\right) E_x = \frac{\omega^2}{c^2} 4\pi \chi_{xx} E_x(0)$$

$$-P_y S E_z + S^2 E_y - \frac{\omega^2}{c^2} K_B E_y = \frac{\omega^2}{c^2} 4\pi \chi_{yy} E_y(0)$$

$$-S P_y E_y + P_y^2 E_z - \frac{\omega^2}{c^2} K_B E_z = \frac{\omega^2}{c^2} 4\pi \chi_{zz} E_z(0)$$

$E_z(0) = 0$ by symmetry,

$$\begin{pmatrix} S^2 - \frac{\omega^2}{c^2} K_B & -P_y S \\ -S P_y & P_y^2 - \frac{\omega^2}{c^2} K_B \end{pmatrix} \begin{pmatrix} E_y \\ E_z \end{pmatrix} = \begin{pmatrix} 4\pi \frac{\omega^2}{c^2} \chi_{yy} E_y(0) \\ 0 \end{pmatrix}$$

$$E_z = \frac{S P_y}{\beta^2} E_y$$

Where $$\beta^2 = P_y^2 - \frac{\omega^2}{c^2} K_B$$

$$\left(\frac{-P_y^2 S^2}{\beta^2} + S^2 - \frac{\omega^2}{c^2} K_B\right) E_y(P, S) = \frac{\omega^2}{c^2} 4\pi \chi_{yy} E_y(0)$$

$$E_y(P,S) = \frac{4\pi \frac{\omega^2}{c^2} \chi_{yy} E_y(0)}{\left\{S^2\left(1 - \frac{P_y^2}{\beta^2}\right) - \frac{\omega^2}{c^2} K_B\right\}} = \frac{\frac{\omega^2}{c^2} 4\pi \chi_{yy} E_y(0) \beta^2}{S^2\left(-\frac{\omega^2}{c^2} K_B\right) - \frac{\omega^2}{c^2} K_B \beta^2}$$

$$E_y(P,z) = \frac{\omega^2}{c^2} 4\pi \chi_{yy} E_y(0) \frac{1}{2\pi} \frac{-1}{\left(\frac{\omega^2}{c^2} K_B\right)} \cdot \beta^2 \int_{-\infty}^{\infty} \frac{e^{-iSz}}{(S^2 + \beta^2)} dS$$

$$E_y(P,z) = \frac{-2\pi \chi_{yy} \beta}{K_B} E_y(0) e^{-\beta |z|}$$

$$E_y(P,0) = \frac{-2\pi \chi_{yy} \beta}{K_B} E_y(0) \longrightarrow \frac{-2\pi \chi_{yy} \beta}{K_B} = 1$$

$$\boxed{\chi_{yy} = -\frac{K_B}{2\pi\beta}}$$

$$E_x(\rho, s) = \frac{\omega^2}{c^2} \cdot \frac{4\pi\chi E_x(0)}{(\rho_y^2 + s^2 - \frac{\omega^2}{c^2}K_B)}$$

$$E_x(\rho, z) = E_x(0)\frac{\omega^2}{c^2} \cdot 4\pi\chi_{xx}\frac{1}{2\pi}\int_{-\infty}^{\infty} ds \; \frac{e^{-isz}}{(\rho_y^2 + s^2 - \frac{\omega^2}{c^2}K_B)}$$

$$E_x(\rho, z) = \frac{\omega^2}{c^2}\, 4\pi\chi_{xx} E_x(0) \cdot \frac{1}{2\pi}\int_{-\infty}^{\infty} ds \; \frac{e^{-isz}}{s^2 + \beta^2}$$

$$= 2\pi\frac{\omega^2}{c^2}\chi_{xx}\frac{1}{\beta}\, E_x(0)\, e^{-\beta|z|}$$

$$E_x(\rho, 0) = \frac{2\pi}{\beta}\cdot\frac{\omega^2}{c^2}\,\chi_{xx}\, E_x(0) \quad \rightarrow \quad \frac{2\pi}{\beta}\cdot\frac{\omega^2}{c^2}\cdot\chi_{xx} = 1$$

$$\boxed{\chi_{xx} = \frac{\beta}{2\pi}\cdot\frac{c^2}{\omega^2}}$$

APPENDIX B

Rough sketch for calculating barrier height

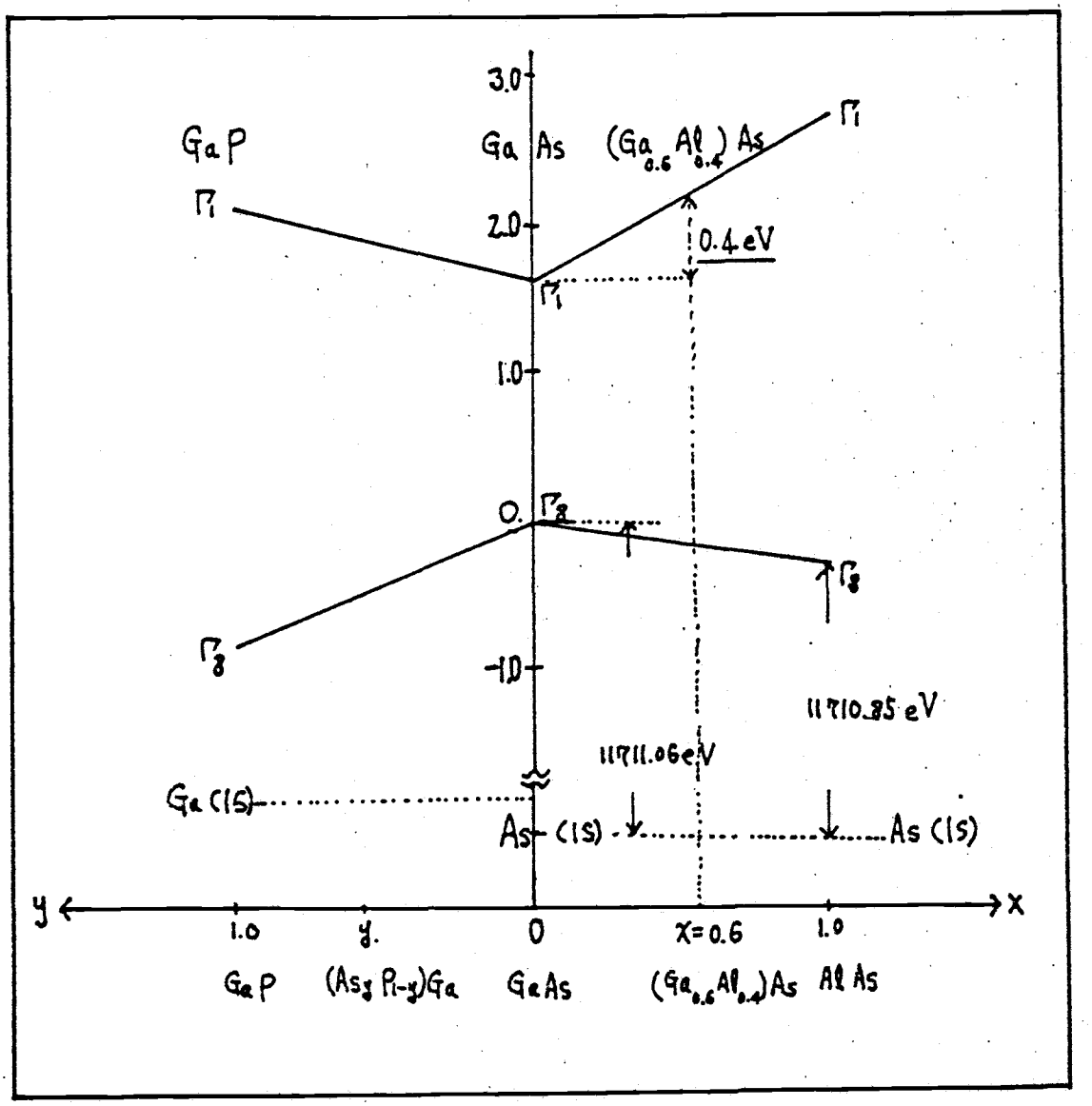

Using the zone center calculated energy band levels Γ_1 and Γ_8 of Ga P, Ga As and Al As (11), we can align their relative positions on a vertical axis using the calculated energy levels of the deep 1s core electron states of Ga and As as reference levels and Γ_8 of Ga As as an arbitrary zero level. Composition is indicated along the horizontal axis where Γ_1 is the conduction band edge and Γ_8 is the top of the valence band edge. From the relative differences of Γ_1 and Γ_8 between Ga As and Ga P or Al As or their alloys, we can determine the energy discontinuities (barrier height at the heterofunction interfaces) ΔE_c and ΔE_v of the conduction and valence bands. For example, to estimate the barrier height E_c of $Ga_xAl_{1-x}As$ alloy with (x=0.6). (1) Draw a vertical line passing through x=0.6. (2) Then we find that ΔE_c is 0.4eV from the graph. That is in good agreement with the experimental values from the optical absorption measurements (22).

APPENDIX C

Two dimensional Fourier transform of the Coulomb potential

$$V(\rho, z) = \frac{e^2}{\epsilon (\rho^2 + z^2)^{1/2}} \qquad (C.G.S)$$

$$V(q_\rho, q_z) = \int dz \int d\varphi \int d\rho \; \rho \; \frac{e^{-i\vec{q}_\rho \cdot \vec{\rho}} \; e^{-i q_z z}}{\epsilon (\rho^2 + z^2)^{1/2}} \cdot e^2$$

Expressed $$e^{-i\vec{q}_\rho \cdot \vec{\rho}} = e^{-i q_\rho \rho \cos\varphi} = J_0(q_\rho \rho)$$

$$- i\, 2 \cos\varphi \, J_1(q_\rho \rho) + \cdots\cdots$$

Only first term survives in the integral

$$V(q_\rho, q_z) = 2\pi e^2 \int_{-\infty}^{\infty} dz \int_0^{\infty} d\rho \; \rho \frac{J_0(q_\rho \rho)}{\epsilon (\rho^2 + |z|^2)^{1/2}} \; e^{-i q_z z}$$

$$= 2\pi e^2 \int_{-\infty}^{\infty} dz \; \frac{e^{-q_\rho |z|}}{\epsilon q_\rho} \; e^{-i q_z z} \qquad (N.N.\ Lebedev\ P.133)$$

$$V(q_\rho, z) = \frac{2\pi e^2 e^{-q_\rho |z|}}{\epsilon q_\rho}$$

APPENDIX D

Derivation of the polarization in the finite temperature

$$\hat{H} = H_0 + H' \tag{D-1}$$

where

H_0 is time independent

H' is time dependent and contains the perturbing potential

H_0, in fact, may contain all the complex interactions among the particles such as electron-electron, electron-phonon, etc. In general, in the Schrödinger picture the density operator is

$$\rho_s(t) = \sum_i \left|\psi_i(t)\right\rangle \omega_i \left\langle\psi_i(t)\right| \tag{D-2}$$

where $\left|\psi_i(t)\right\rangle$ are state functions that satisfy the Schrödinger Equation and setting $\hbar=1$,

$$\hat{H}\left|\psi(t)\right\rangle = i\frac{\partial}{\partial t}\left|\psi(t)\right\rangle \tag{D-3}$$

Defining an interaction picture,

$$\left|\psi_I(t)\right\rangle = e^{iH_0t}\left|\psi_s(t)\right\rangle \tag{D-4}$$

$$\rho_I(t) = e^{iH_0t}\,\rho_s(t)e^{-iH_0t} \tag{D-5}$$

The density operator evolves in time according to

$$\frac{\partial}{\partial t}\rho_I(t) = iH_0\, e^{iH_0t}\,\rho_S(t)\, e^{-iH_0t} + e^{iH_0t}\rho_S(t)$$

$$e^{-iH_0t}\,(-iH_0) + e^{iH_0t}\,\frac{\partial\rho_S}{\partial t}\,e^{-iH_0t} \qquad \text{(D-6)}$$

$$\frac{\partial\rho_S}{\partial t} = \frac{1}{i}\hat{H}\,\left|\psi_i(t)\right\rangle\omega_i\left\langle\psi_i(t)\right| + \left|\psi_i(t)\right\rangle\omega_i\left\langle\psi_i(t)\right|\left(-\frac{\hat{H}}{i}\right) \qquad \text{(D-7)}$$

Combining Eq. (D-6) and Eq. (D-7),

$$\frac{\partial\rho_I}{\partial t} = -i\, e^{iH_0t}\, H'\, e^{-iH_0t}\, e^{iH_0t}\,\left|\psi_i\right\rangle\omega_i\left\langle\psi_i\right| e^{-iH_0t}$$

$$+ie^{iH_0t}\left|\psi_i\right\rangle\omega_i\left\langle\psi_i\right| e^{-iH_0t} e^{iH_0t}\, H' e^{-iH_0t}$$

$$= -iH_I'(t)\rho_I + i\rho_I(t)H_I' = i[\rho_I(t),\, H_I'(t)]$$

$$\frac{\partial\rho_I}{\partial t} = i[\rho_I(t),\, H_I'(t)] \qquad \text{(D-8)}$$

Now write a formal exact solution

$$\rho_I(t) = \rho_I(-\infty) + i\int_{-\infty}^{t}[\rho_I(t'),\, H_I'(t')]dt'$$

where $\rho_I(-\infty)$ is the density operator before the H' is turned on. Thus

$$\rho_I(-\infty) = \frac{e^{-\beta(H-\mu N)}}{\mathrm{Tr}\; e^{-\beta(H-\mu N)}}$$

Now iterate once (or as many terms as a non-linear may demand)

$$\rho_I(t) = \rho_I(-\infty) + i \int_{-\infty}^{t} [\rho_I(-\infty), H'_I(t')]dt'$$

Now it can be observed, that with respect to the total system without the external potential, the interaction picture is the Heisenberg picture, which is the common picture for expressing the Green's functions, and we can, with this understanding, drop the subscript I but making certain we are not ignoring its original meaning. Thus we can finally write, when the time dependent interaction is of the form

$$H'(t) = \int \psi^+(x',t) V_{int}(x',t) \psi(x',t)\, dx'$$

(where spin indices are suppressed) where the field operators are in the Heisenberg picture as defined just above, that the average value of operator, $\theta(t)$ also in the Heisenberg picture, is

$$\langle\theta\rangle = \mathrm{Tr}\ \rho\ \theta$$

$$= \mathrm{Tr}\ (\rho(-\infty)\,\theta) + i\ \mathrm{Tr}\{\int dx' \int_{-\infty}^{t} V_{int}(x',t')$$

$$[\rho(-\infty), \psi^+(x',t')\psi(x',t')]\theta(x,t)$$

Finally since the trace is invariant to cyclic permutation we have using $\rho(-\infty)=\rho_0$

$$\langle\theta\rangle = \mathrm{Tr}(\rho_0\theta)+i\ \mathrm{Tr}\int dx' \int_{-\infty}^{t} dt'\ V(x',t')\ \rho_0$$

$$[\psi^{+}(x',t')\psi(x',t'),\theta(x,t)]$$

Now, if θ is the density whose mean value we need, then $\theta(x,t) = \Psi^{+}(x,t)\Psi(x,t)$ so that finally in coordinate representation

$$\langle\theta\rangle = \langle\theta\rangle_0 - i\int dx' \int_{-\infty}^{\infty} dt'\ V(x',t')D_R(x,\varepsilon;x',\varepsilon')$$

where

$$D_R(x,t;x',t') = \langle \mathrm{tr}\ \rho_0[\psi^{+}(x,t)\psi(x,\varepsilon),\psi^{+}(x',t')\psi(x',t')]\rangle$$

$\tilde{\theta}(t-t')$, $\tilde{\theta}$ = Heaviside function

is called a retarded Green's Function. The retarded Green's function is difficult to calculate directly and instead the time ordered Green's function (polarization)

$$\Pi(x,t\ x',t') = \ll T\{\psi^{+}(x,t)\psi(x,t)\psi^{+}(x',t')\psi(x',t')\}\gg$$

is calculated (the double bracket is the statistical avrage). This time ordered Green's function is connected to the retarded Green's function by the Fluctuation Dissipation theorem (28). For our purposes, we need only to calculate the time ordered Green's function since it contains the same collective modes (i.e. same singular structure) as the retarded Green's function.

In the random phase approximation, the polarization can be expressed as the following set of Feynman diagrams:

$\Pi(x,x';\xi)$ =

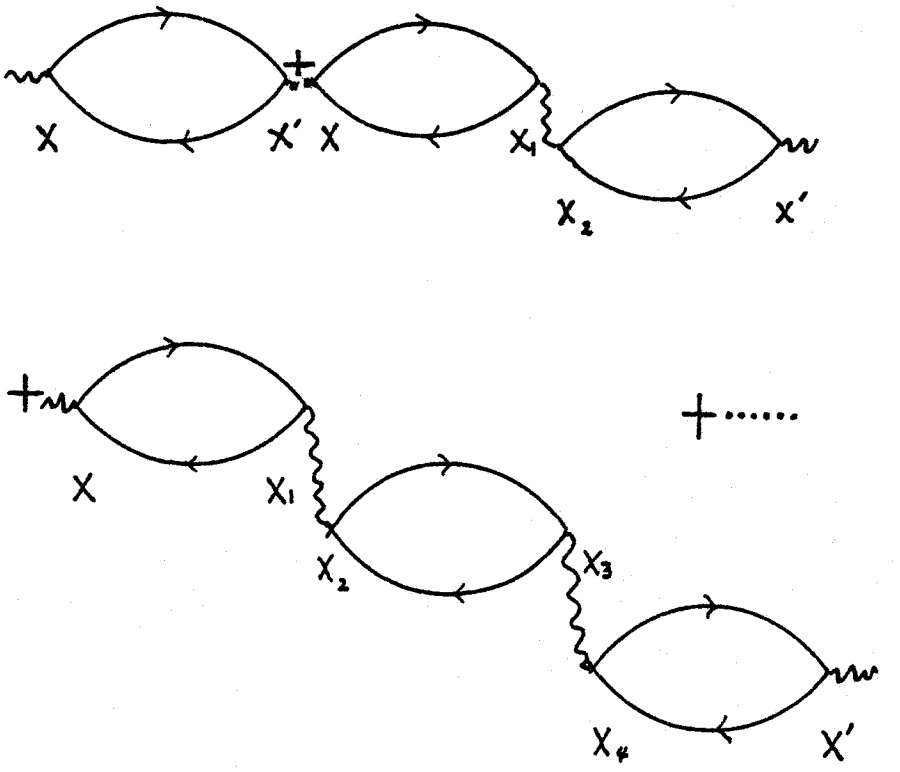

where

$x \equiv (x,t)$

Final state interactions, which are expected to be of importance in intersubband transitions. have been neglected.

APPENDIX E

Using Fourier integral,

$$\frac{1}{q^2 + (q_z + G)^2} = \frac{1}{2q} \int_{-\infty}^{\infty} dz\, e^{i(q_z + G)z}\, e^{-q|z|}$$

$$= \frac{1}{2q} \int_{-\infty}^{\infty} dz\, e^{i q_z \cdot z}\, e^{-q|z|}\, e^{i G z}$$

Then,

$$\sum_G \frac{1}{q^2 + (q_z + G)^2} = \frac{1}{2q} \int_{-\infty}^{\infty} dz\, e^{i q_z z}\, e^{-q|z|} \sum_G e^{iGz}$$

The sum over G defines a periodic function of Z with period (a+d).

$$\sum_G e^{iG\cdot z} = (a+d) \sum_l \delta(z - z_l)$$

$$\sum_G \frac{1}{q^2 + (q_z + G)^2} = \frac{(a+d)}{2q} \int_{-\infty}^{\infty} dz\, e^{i q_z z}\, e^{-q|z|} \sum_l \delta(z - z_l)$$

$$= \frac{(a+d)}{2q} \sum_l \exp\left[i q_z z_l - q|z_l| \right]$$

Where $z_l = l(a+d)$,

$$= \frac{(a+d)}{2q} \left\{ \sum_{l=0}^{\infty} \exp\left[i q_z z_l - q z_l \right] + \sum_{l=1}^{\infty} \exp\left[-i q_z z_l - q z_l \right] \right\}$$

$$= \frac{(a+d)}{2q} \left\{ \frac{\sinh q(a+d)}{\cosh q(a+d) - \cos q_z (a+d)} \right\}$$